Magnetorheological Strut for Vibration Isolation System of Space Launcher

Author:

Ing. Ondřej Macháček

Supervisors:

Doc. Ing. Ivan Mazůrek, CSc.

Ing. Jakub Roupec, PhD.

INSTITUTE OF **MACHINE**
AND **INDUSTRIAL DESIGN**

Brno, 7 December, 2018

Content and Motivation

Content

- State of art
- Aim of thesis
- Methods
- Results
- Conclusion

Spacecraft (Payload)

Vibration Isolation System (VIS)

1 kg on orbit = 4 000 – 39 000 USD

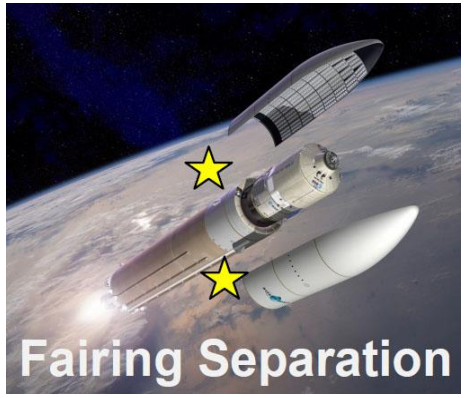

State of art

Structural vibration isolation systems (VIS) – Payload adapters

- **Low efficiency** → **VIS based on struts**

[Perez, 2014]

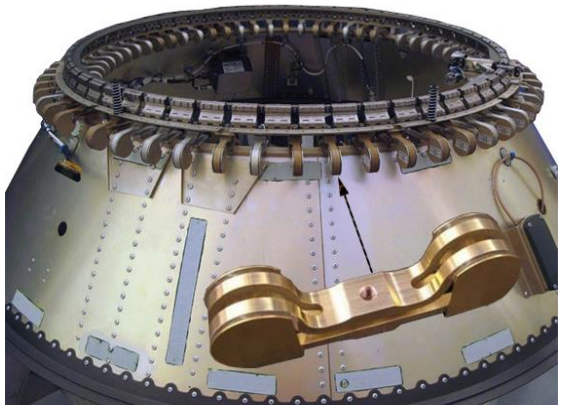

[White, 2015]

[spacex.com]

State of art

Vibration isolation systems based on struts – Stewart platform

Passive

[Rubsamen, 2003]

Active

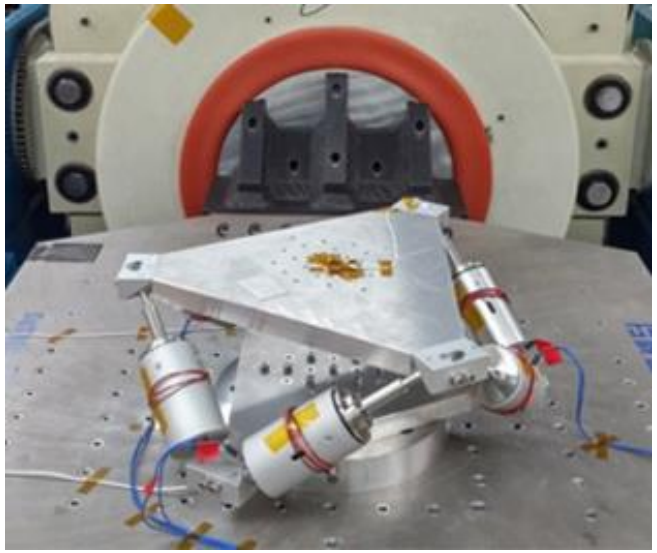

[Lee, 2015]

Semi - active

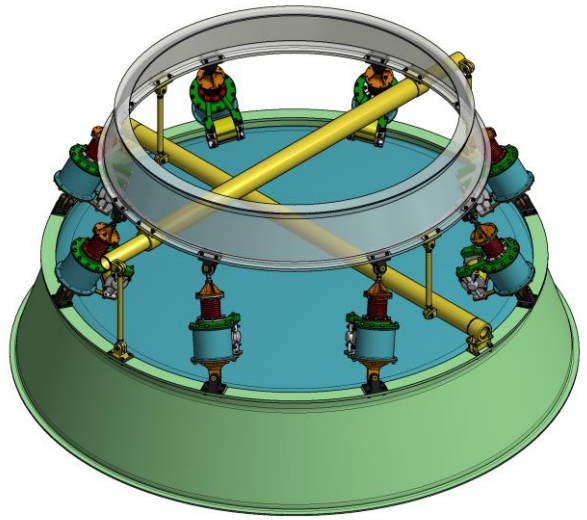

[esa.com]

State of art

Transmissibility comparison of Passive, Active and SA vibration isolators (axial)

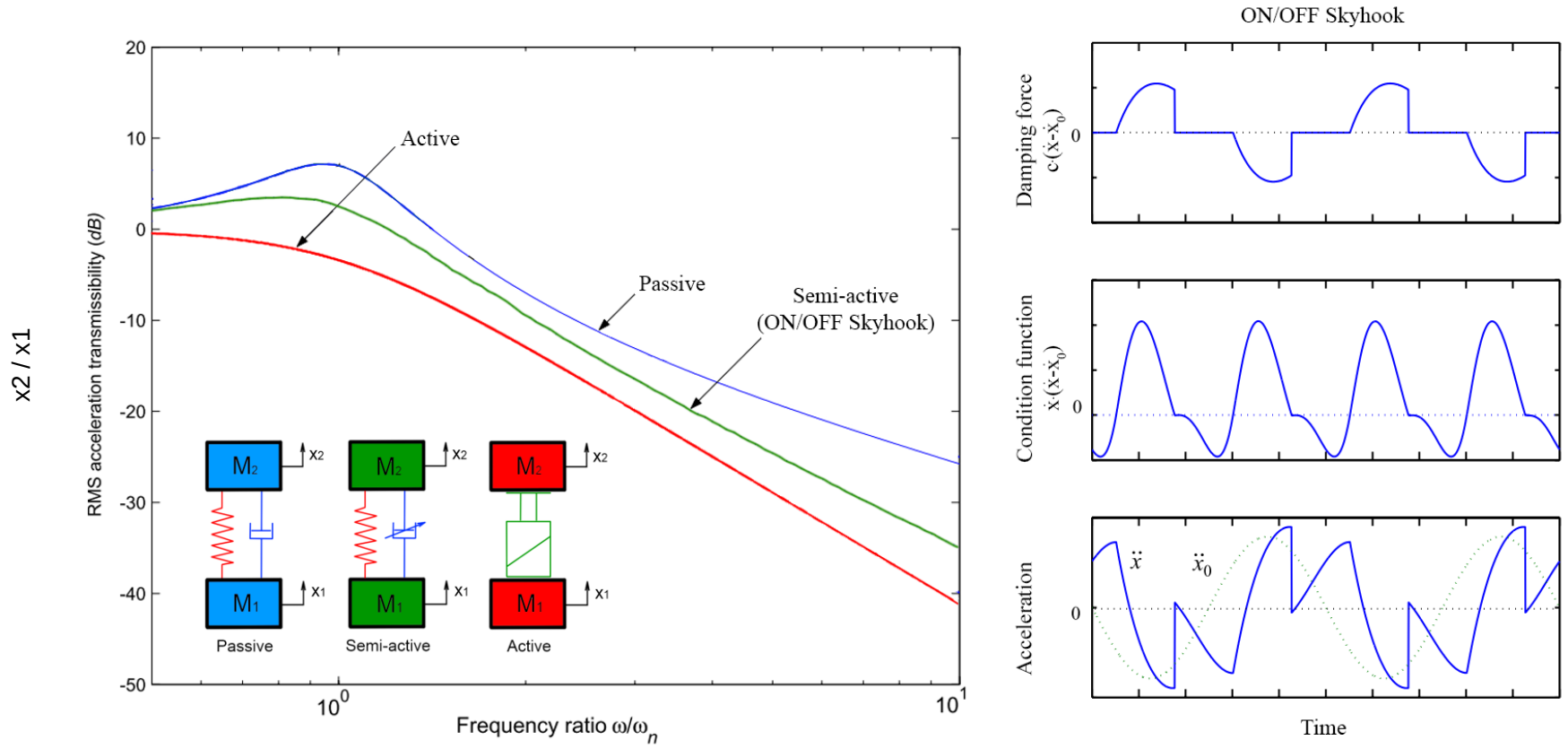

[Liu, 2005]

State of art

Transmissibility comparison of Passive, VIS with and without stabilizer (lateral)

No stabilizer

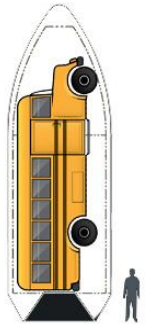

http://www.spacex.com

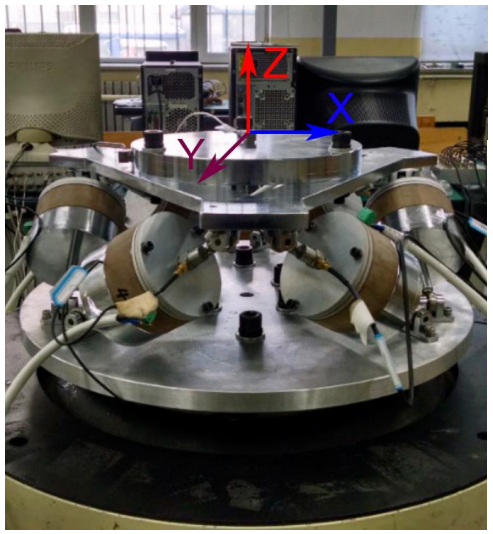

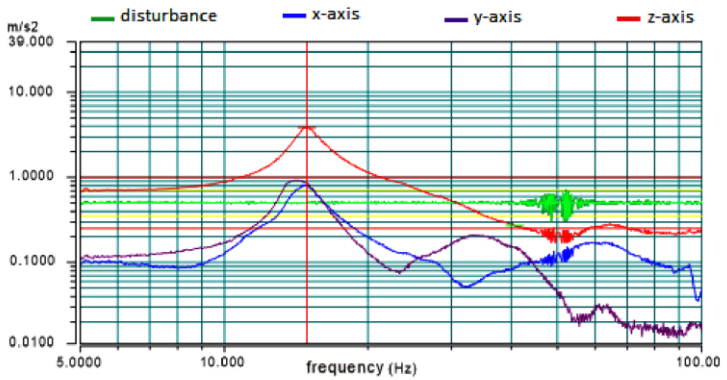

[Chi, 2015]

Hydraulic stabilizer

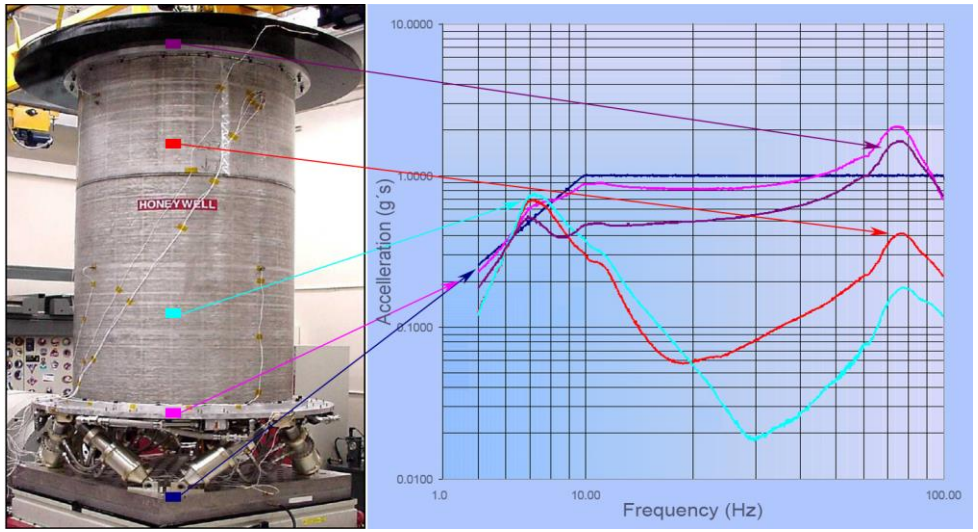

[Ruebsamen, 2003]

State of art

Hydraulic stabilizer of Evolved Launch Vibration Isolation System (ELVIS)

Usually shaped spacecrafts (payloads) are prone to yawing

Lateral direction has to be stiff

- Strut position
- Stabilizer

High damping in axial direction →

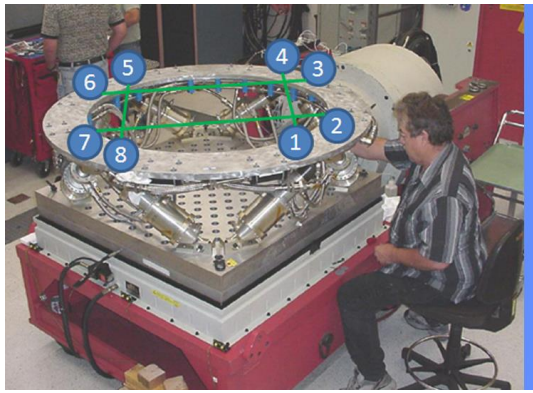

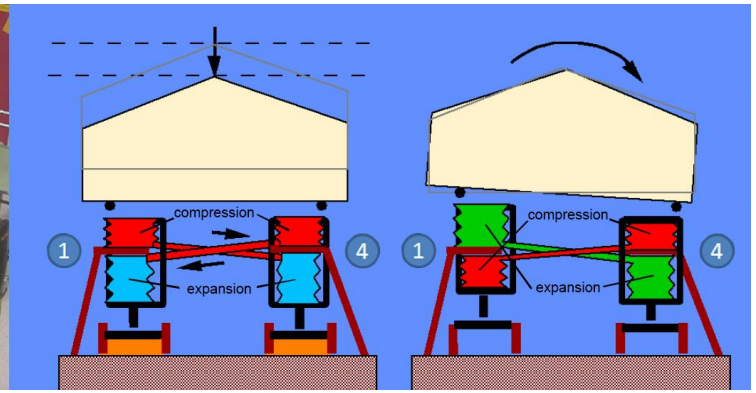

[Ruebsamen, 2003]

Torsion stabilizer

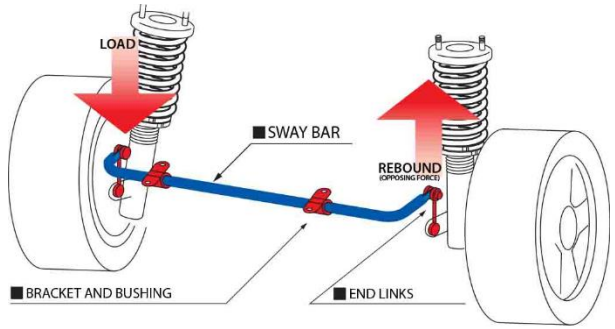

http://www.cuscousainc.com

State of art

Struts of VIS for launch vehicle

No leakage ⟶ **unconventional sealing by elastic metal bellows**

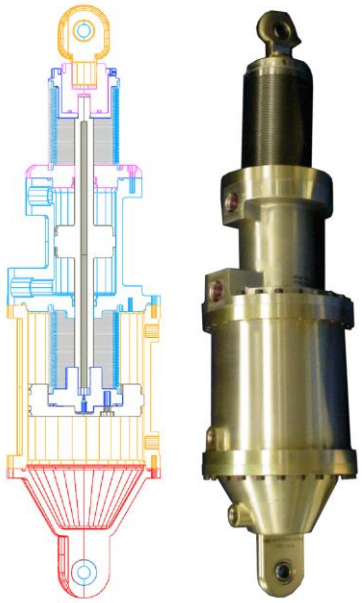

[Rubsamen, 2003]

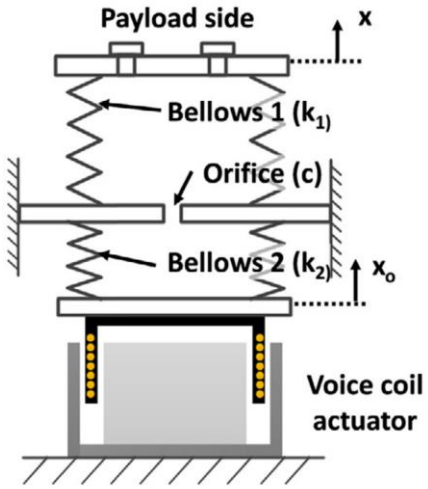

[Lee, 2015]

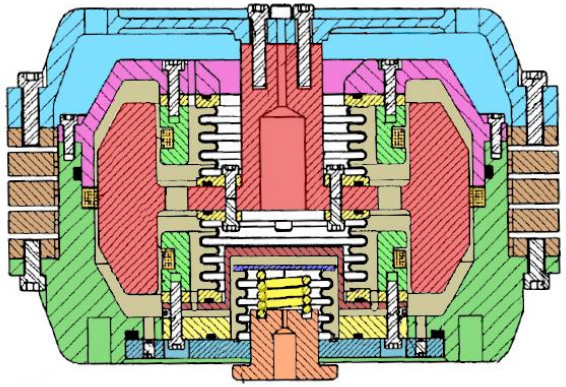

[Kelso, 2004]

State of art

Elastically connected damper

[Harris, 2002]

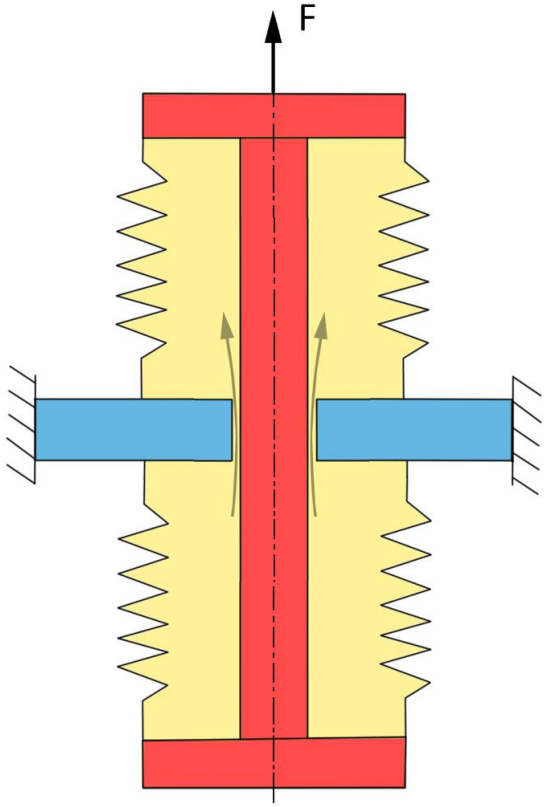

Low damping

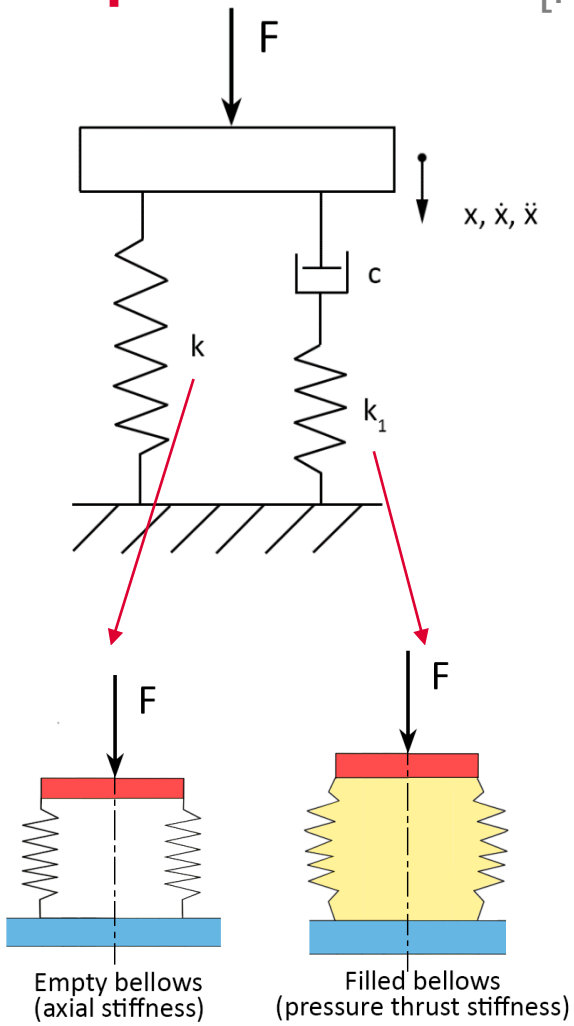

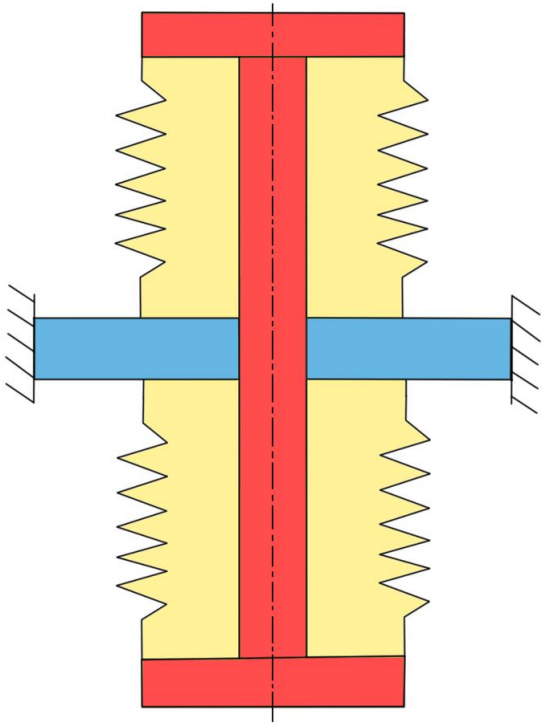

High damping

State of art

Elastically conneceted damper

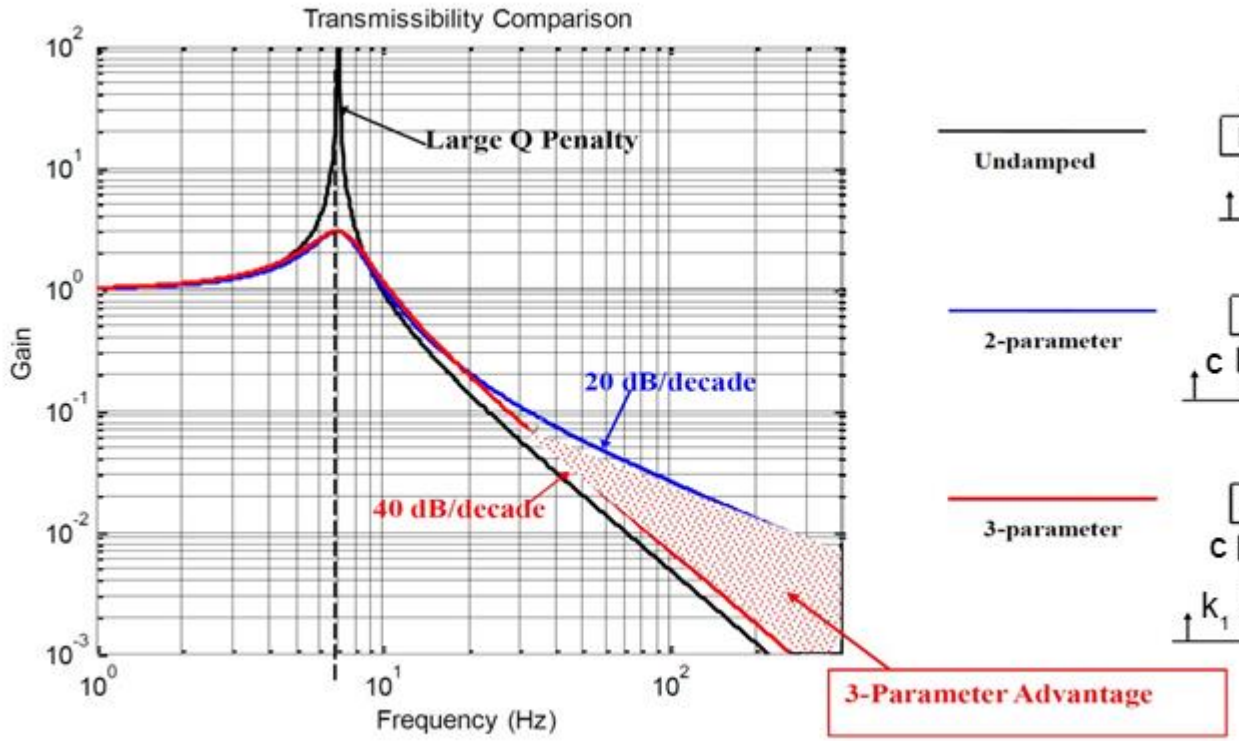

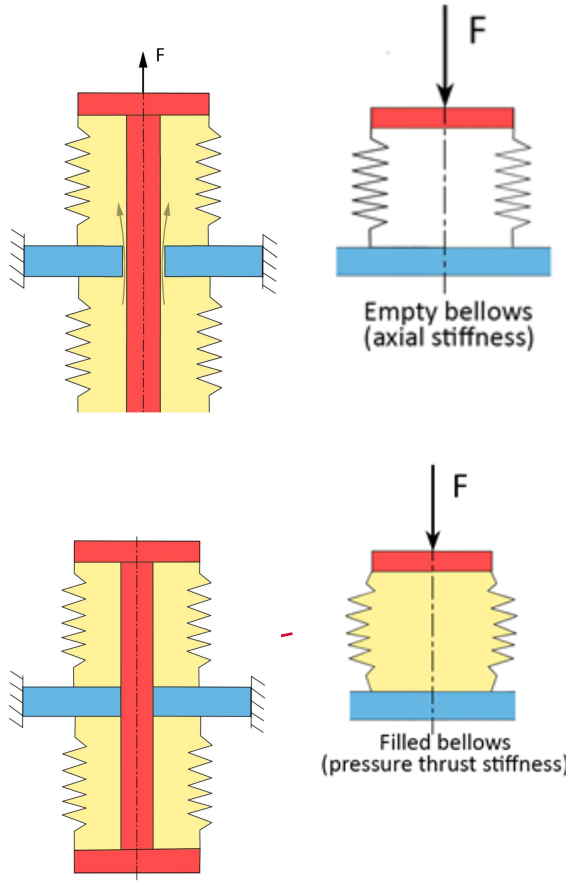

Available in product list

Unavailable in product list

State of art

Magnetorheological damper (MR)

Controllable damping force

Effective semi-active control → high **Dynamic force range** & low **response time**

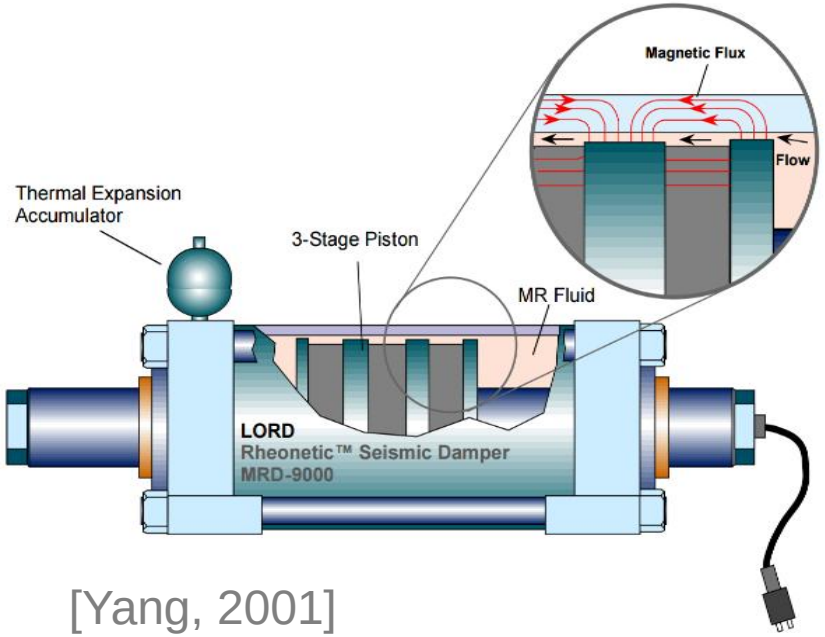

[Yang, 2001]

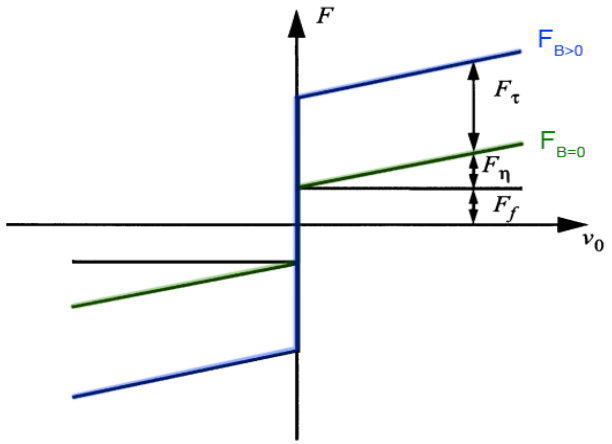

$$D(v,B) = \frac{F_{B=max}}{F_{B=0}}$$

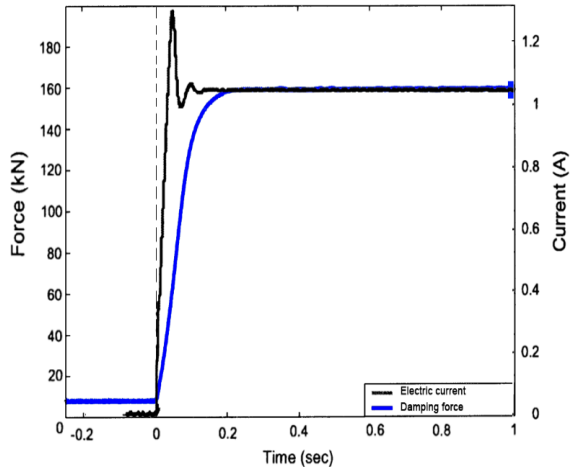

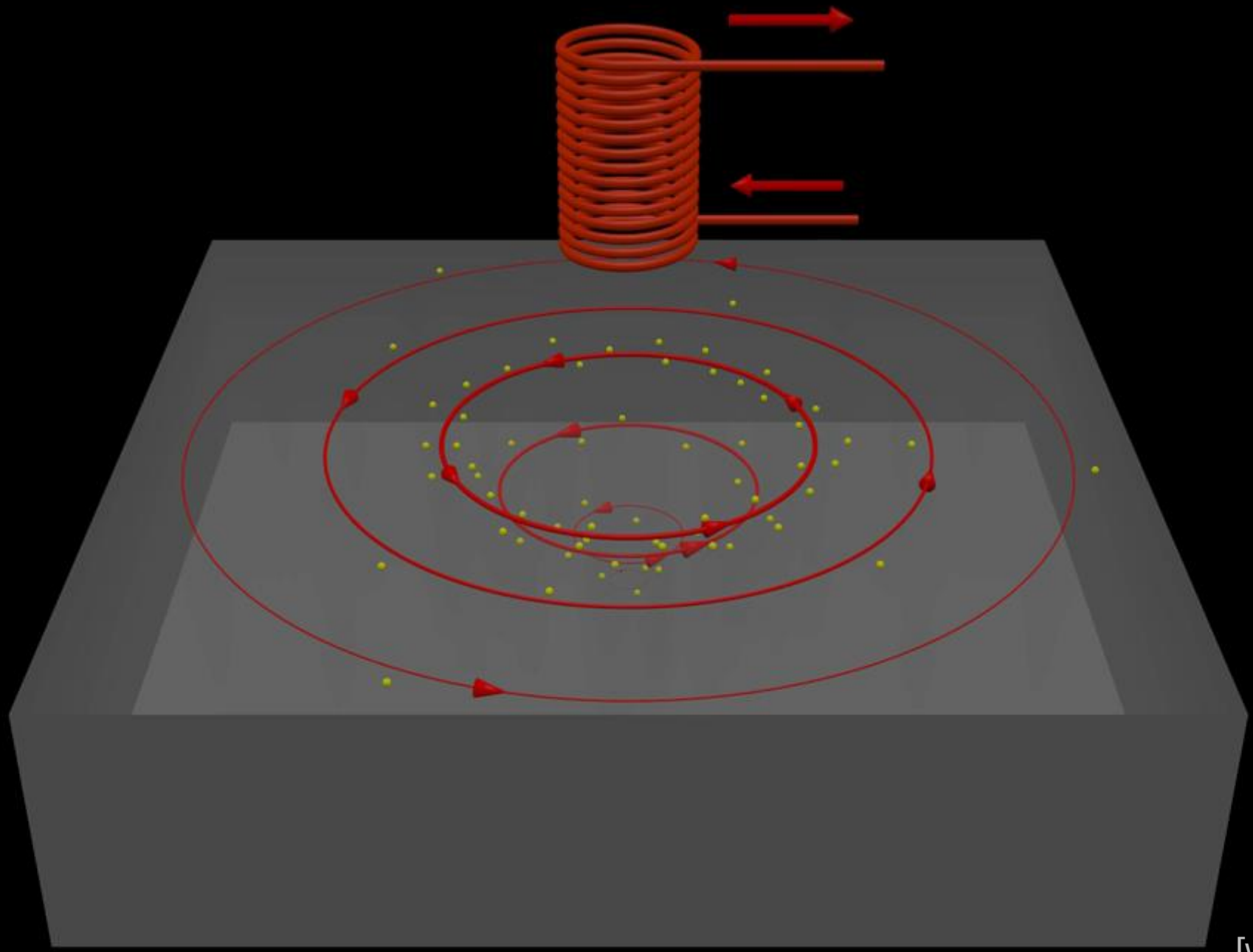

[www.youtube.com]

State of art

Eddy current elimination

Shape approach

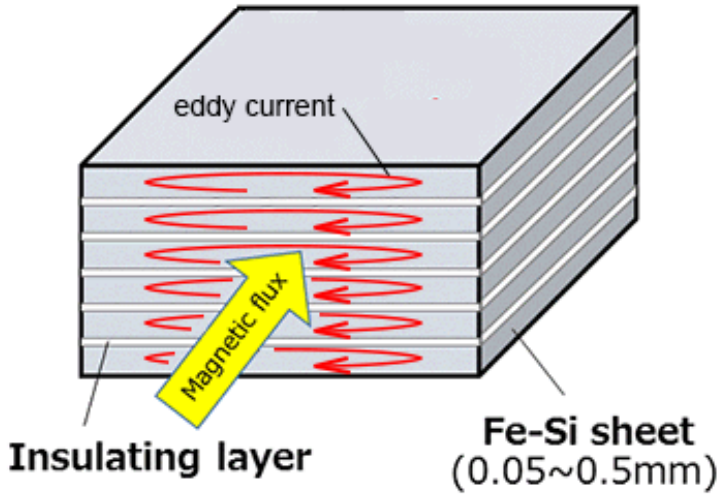

Material approach

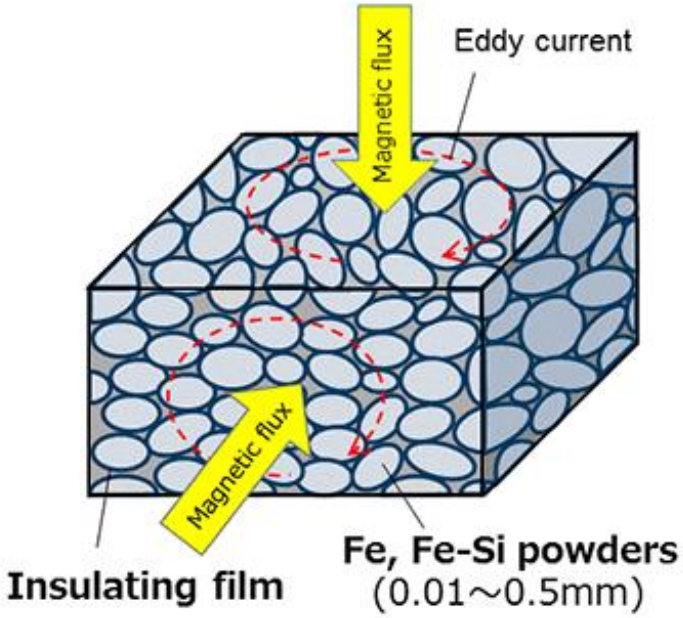

[www.global-sei.com]

Summary of literature review

Type of VIS

- Structural
- Based on struts

Control strategy

- Passive
- Active
- Semi-active (MR damper)

Stabilizer

- Hydraulic
- Mechanical

Sealing

- Sealing cuff
- Metal bellows

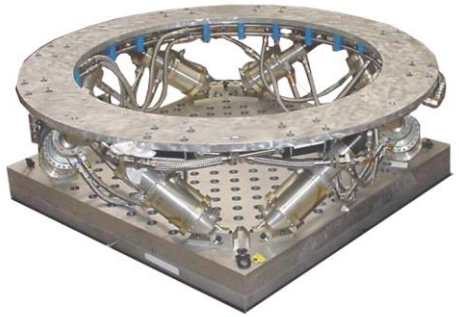

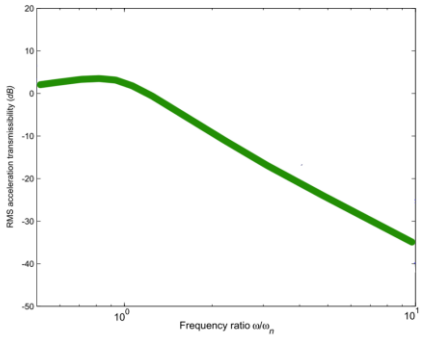

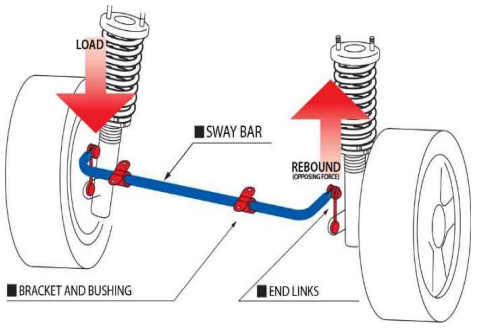

Aim of the thesis

Design of semi-active strut combining spring and damper function for the vibration isolation system of the launch vehicle

Sub aims:

- VIS concept selection
- Determination of single strut load (multibody model)
- Find an optimal parameters of MR damper
- Design dimmensions of struts (several models)
- Experimental strut design
- Tests (the models verification)

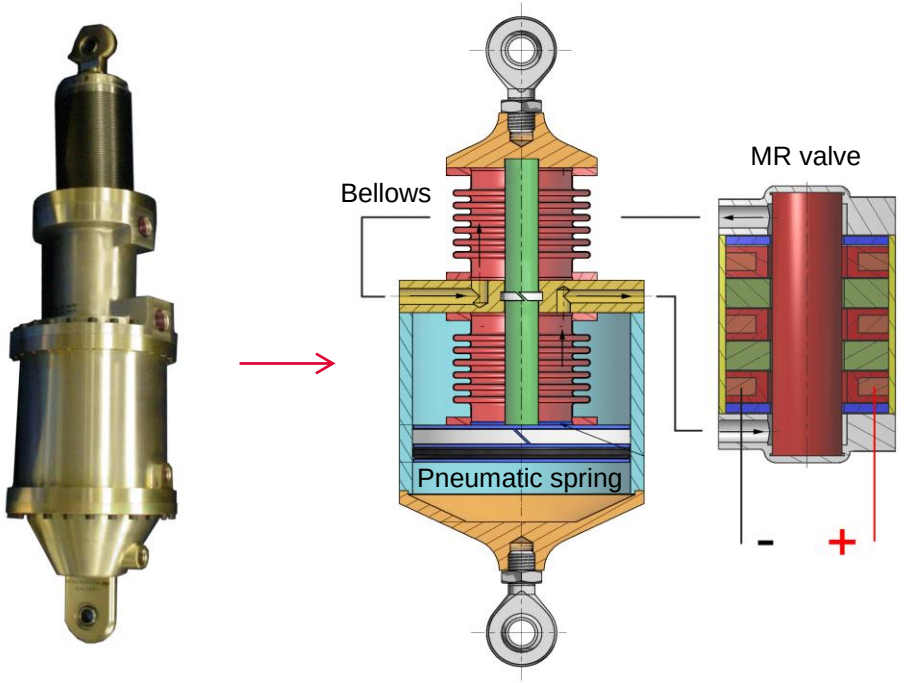

ELVIS strut (passive) → **MR strut (semi-active)**

Methods

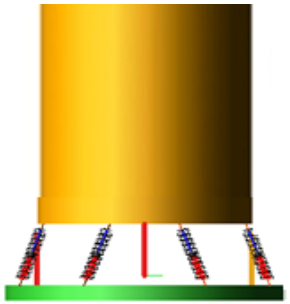

Dimensions, parameters

and loading of single strut

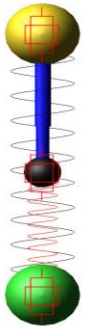

Models verification

Primary (k) and sedondary (k_1) stiffness of the strut

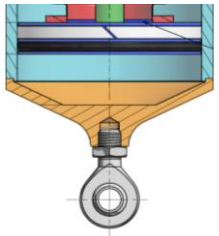

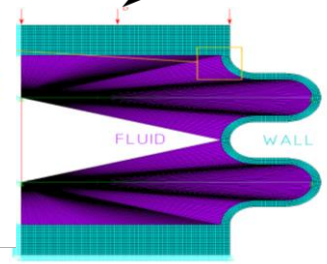

ON / OFF damping

Time response

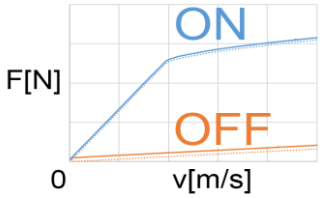

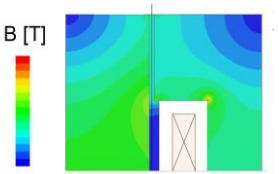

Modifications

Fabrication

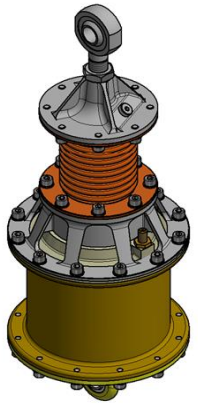

Magnetic circuit dimensions

Channels for MR fluid dimmensions

Strut dimensions

Bellows dimensions

Pneumatic spring dimensions

Dynamic model of VIS

VIS requirements			
Parameter	Symbol	Value	Unit
VIS connection diameter	$øD_B$	1920	[mm]
VIS minimum height	h	390	[mm]
Payload connection diameter	øDP	1280	[mm]
Payload mass	m	1500	[kg]
Payload centre of mass height	hCoG	1500	[mm]
Max. acceleration (lateral)	a_x	±0.9	[g]
Max. acceleration (axial)	a_y	±5.5	[g]
Max. displacement of payload (lateral)	d_x	30	[mm]
Max. displacement of payload (axial)	d_y	10	[mm]

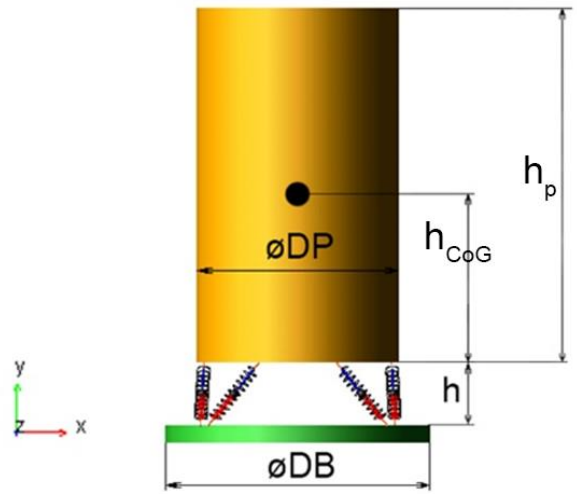

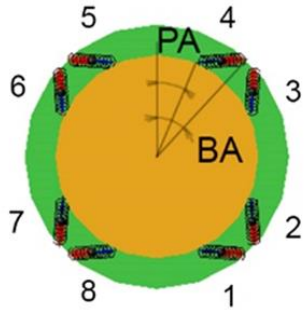

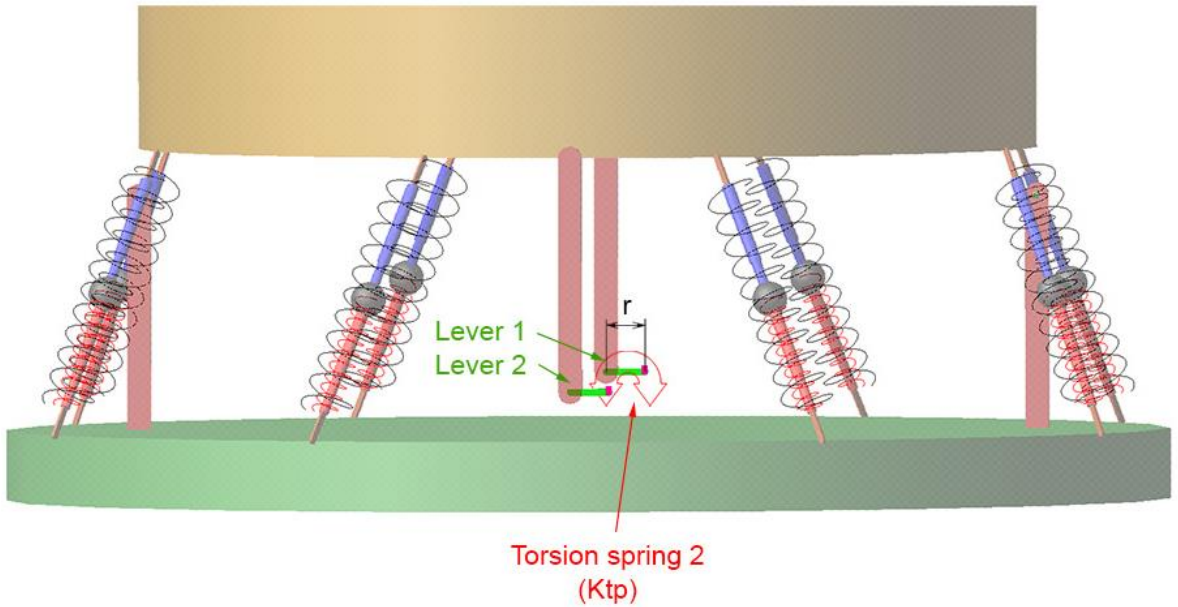

Dynamic model of VIS

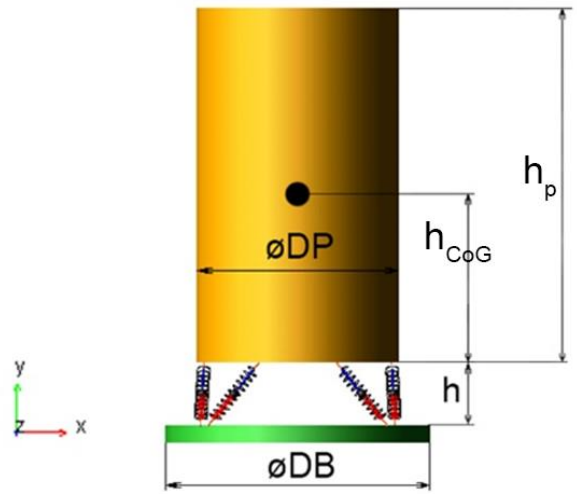

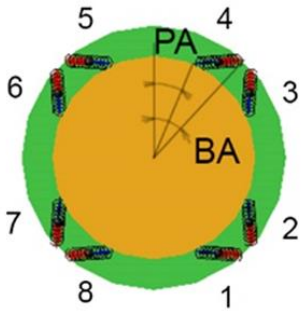

Final configuration

Parameter	Symbol	Value	Unit
Primary stiffness of the strut	k_A	1230	[N/mm]
Damping of the strut	c_A	26	[Ns/mm]
Ratio k_B/k_A	N	50	[-]
Torsion stiffness of stabilizer	k_{MS}	$1.072 \cdot 10^7$	[Nm/rad]
Angle between struts along payload diameter	PA	19	[deg]
Angle between struts along base diameter	BA	26	[deg]
VIS height	h	390	[mm]

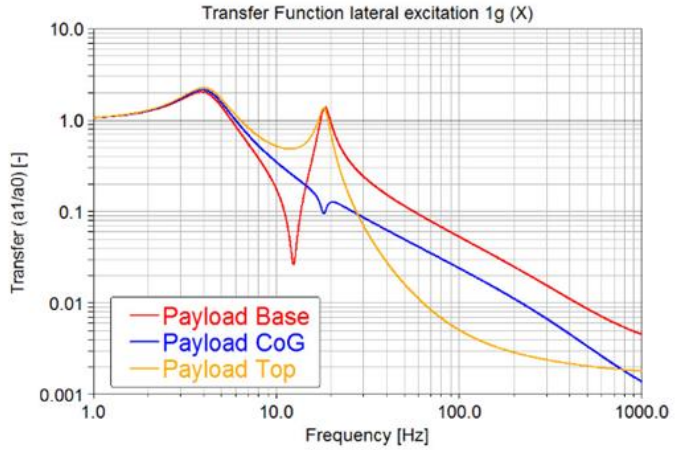

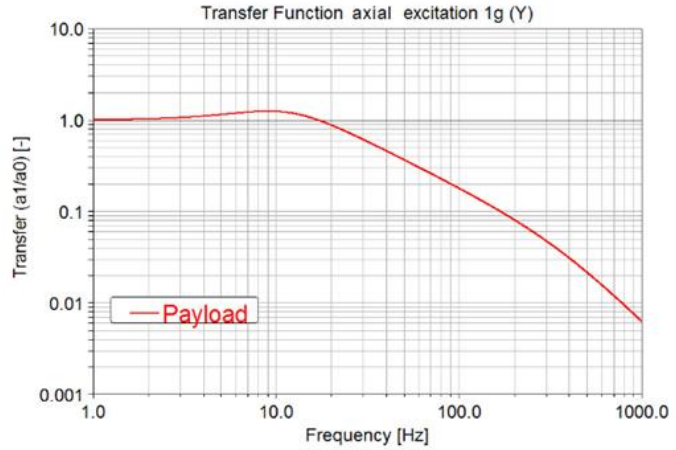

Dynamic model of single strut

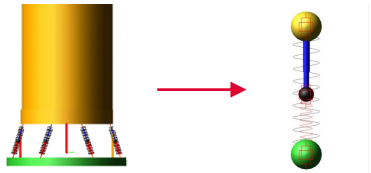

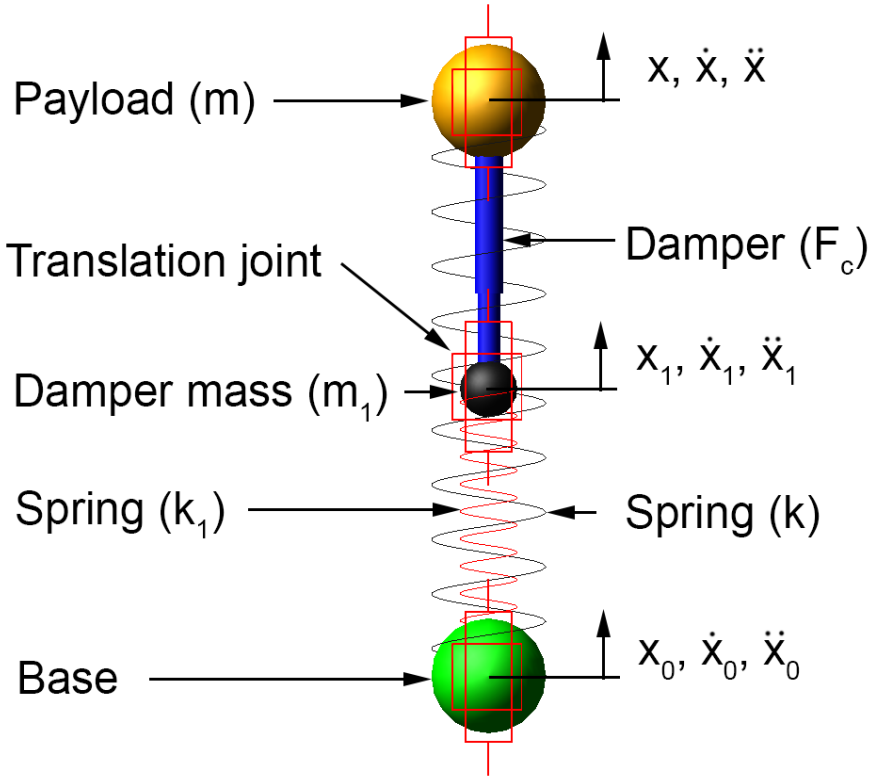

Parameter	Symbol	Value	Unit
Experimental payload mass	m	100	[kg]
Primary stiffness of experimental strut	k	390	[N/mm]
Damping of the strut (activated state)	C_{ON}	12.5	[Ns/mm]
Time response of the damper	t	?	[ms]
Dynamic force range of the damper ($D= C_{ON}/C_{OFF}$)	D	?	[-]
Secondary stiffness of experimental strut	k_1	?	[N/mm]

Semi-active control
(ON/OFF skyhook)

$$\dot{x} \cdot (\dot{x} - \dot{x}_1) \geq 0 \rightarrow Fc = Fc_{max}$$
$$\dot{x} \cdot (\dot{x} - \dot{x}_1) < 0 \rightarrow Fc = Fc_{min}$$

Dynamic model of single strut

Influence of MR damper time response

Semi – active control

Force comparison of fast and slow damper

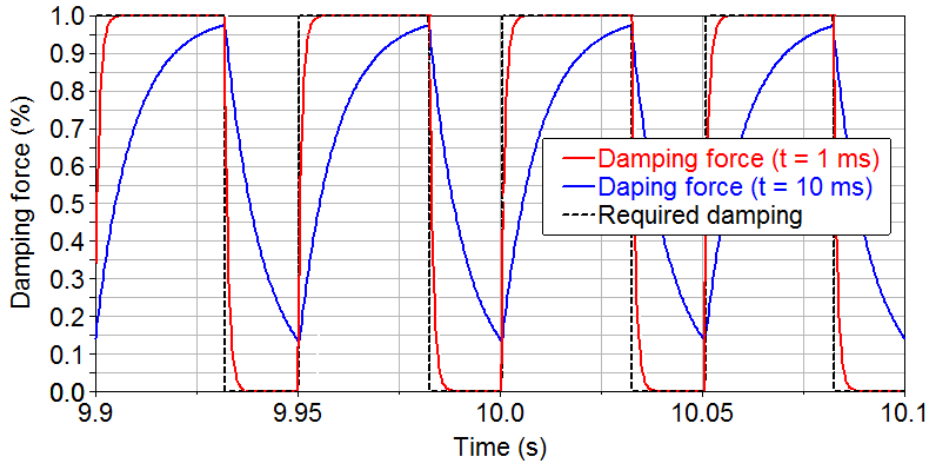

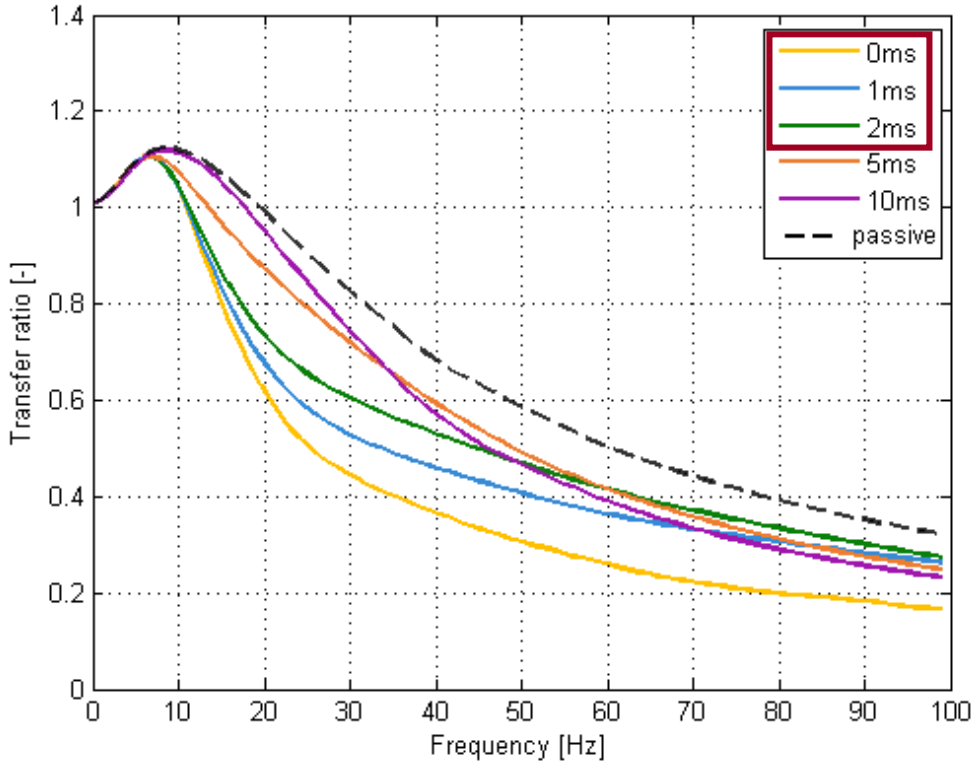

Dynamic model of single strut

Influence of MR damper dynamic force range

Semi – active control

Typical F-v dependency of MR damper

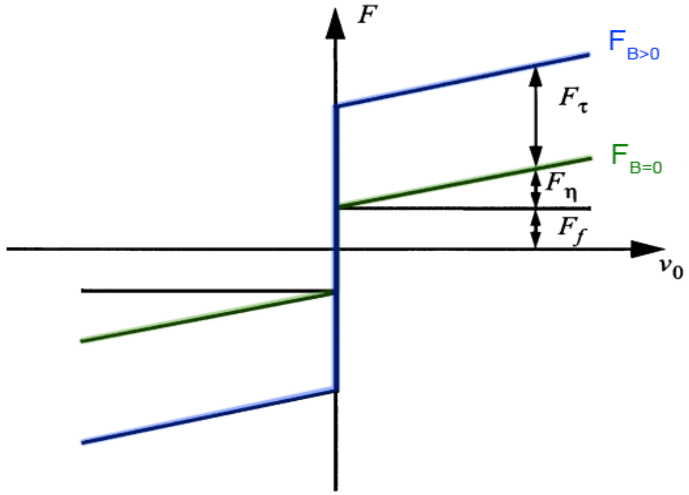

$$D(v,B) = \frac{F_{B=max}}{F_{B=0}}$$

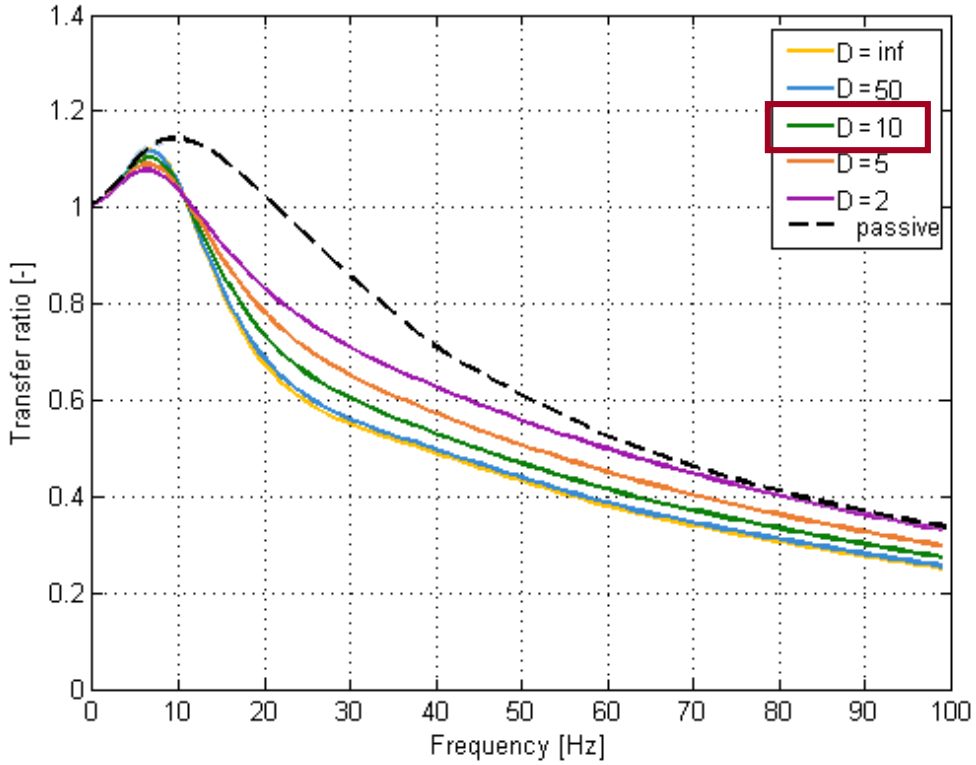

Dynamic model of single strut

Semi – active control

Influence of MR damper secondary stiffness (k_1)

Secondary stiffness

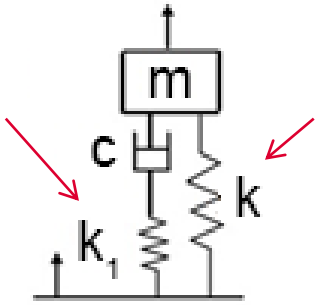

Primary stiffness

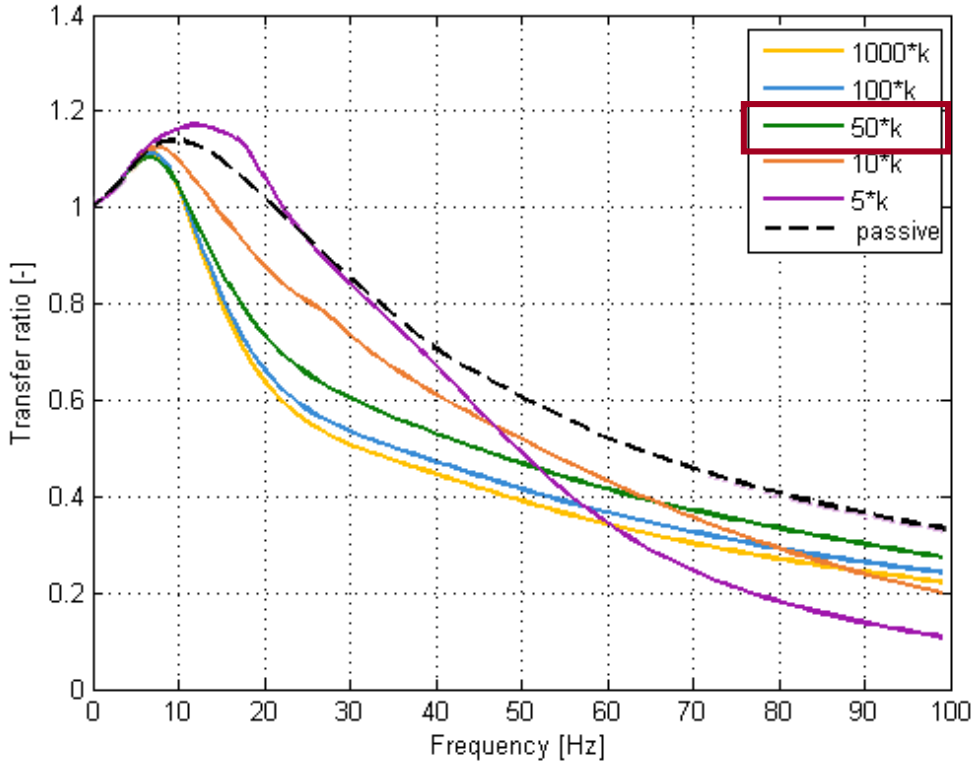

Conclusion of simulations:

Time response: < 2ms
Dynamic force range: approx. 10
Secondary stiffness: k1 = approx 50*k

Experimental strut

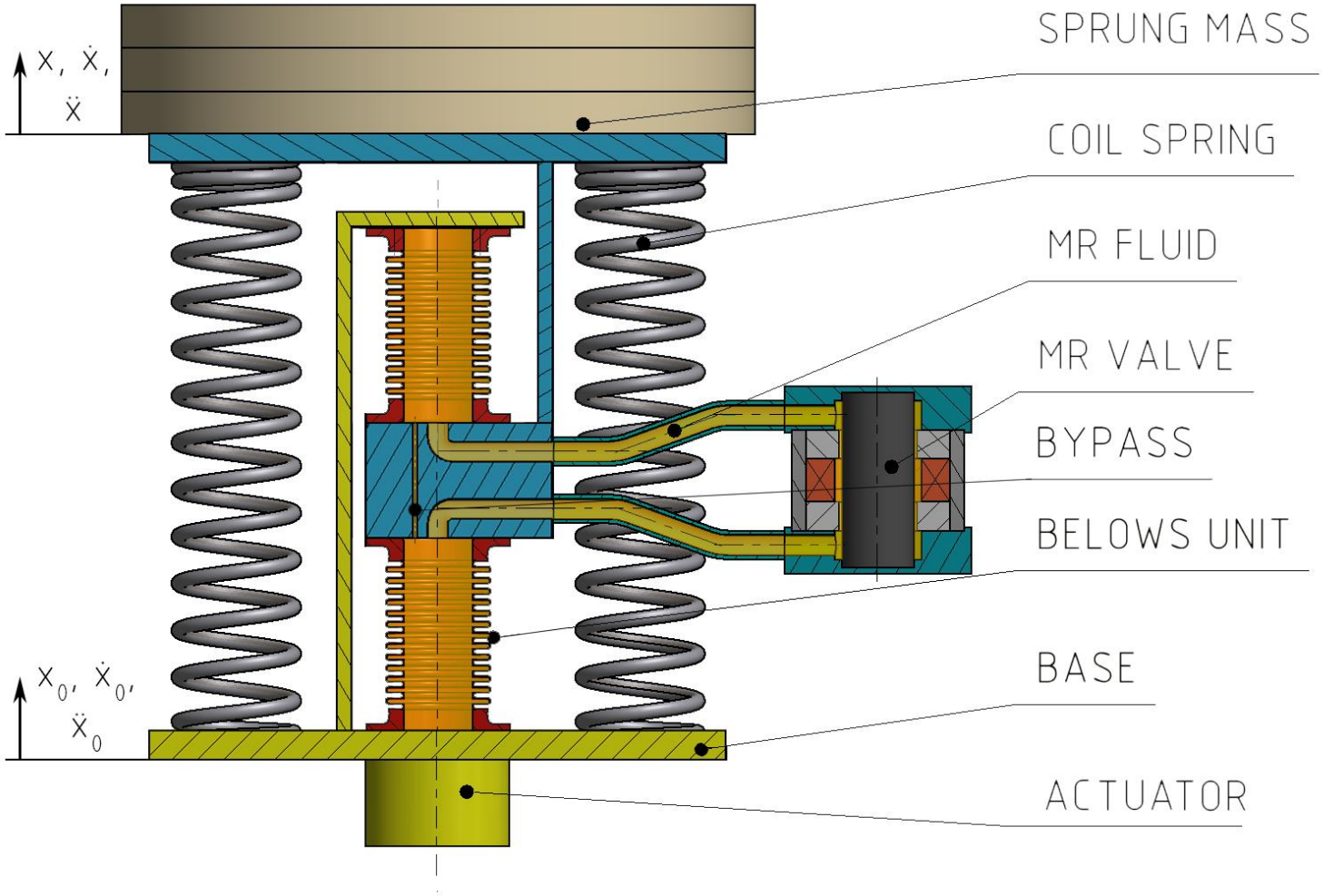

Metal Bellows

FEA of metal bellows was verified by Measurement

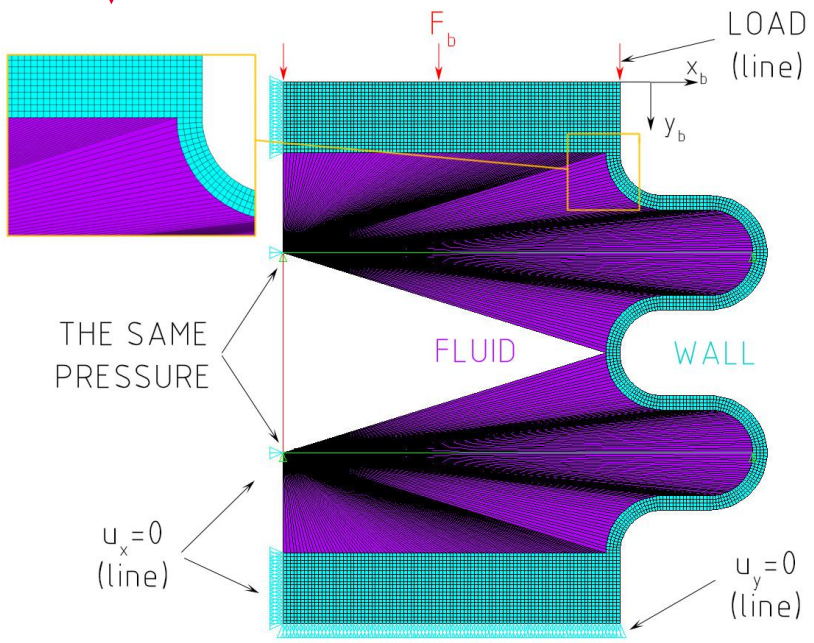

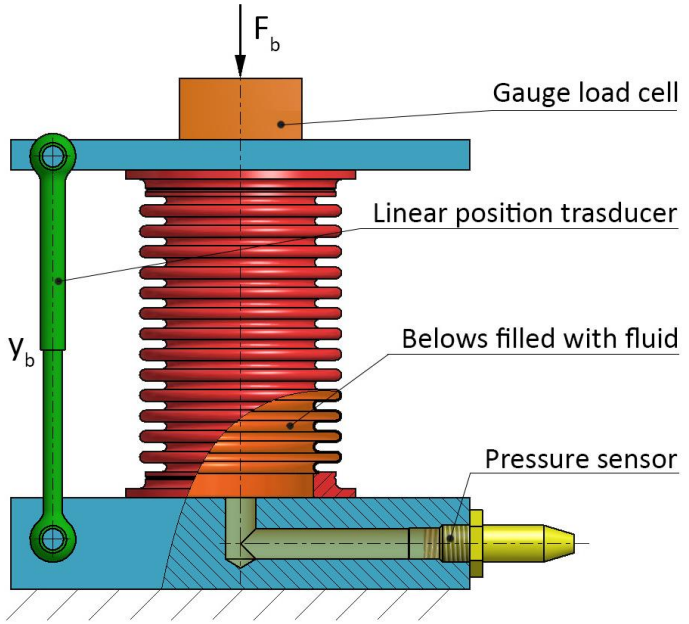

FEA vs simulation: 11 % (axial stiffness); 5.7 % (pressure thrust stiffness)

MR valve design

Hydraulic part

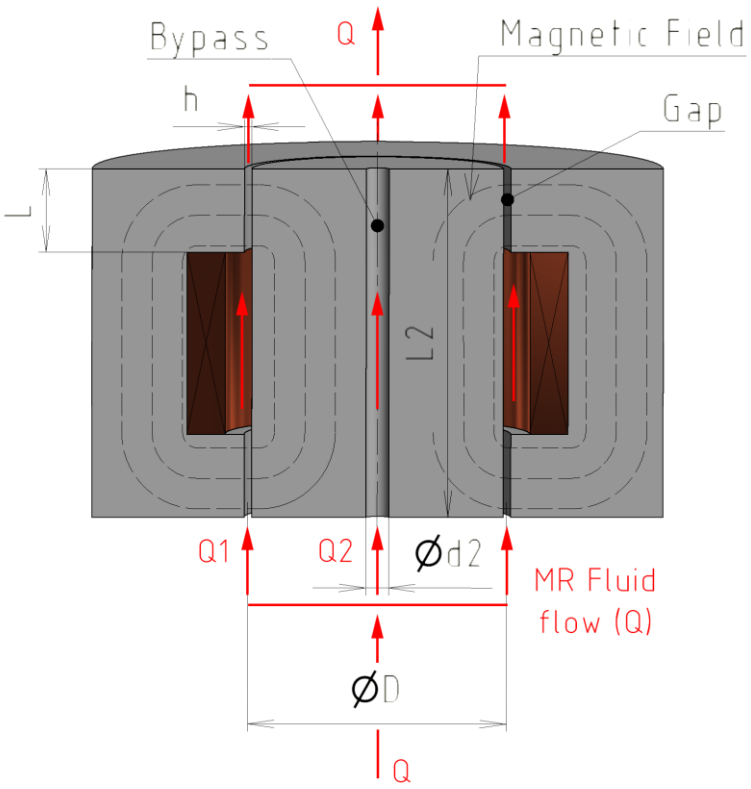

$$F = F_{gap} + F_{bypass}$$

$$F_{gap} = \left(1 + \frac{\pi \cdot D \cdot h \cdot v_0}{2 \cdot Q1}\right) \frac{12 \cdot \eta \cdot Q1 \cdot L \cdot A_p}{\pi \cdot D \cdot h^3} + \mathrm{c} \cdot \frac{\tau_0 \cdot L \cdot A_p}{h} \cdot sgn(v_0)$$

$$F_{bypass} = \left(1 + \frac{\pi \cdot {d_2}^2 \cdot v_0}{8 \cdot Q1}\right) \frac{48 \cdot \eta \cdot Q2 \cdot L2 \cdot A_p}{\pi \cdot {d_2}^4}$$

[Yang, 2001]

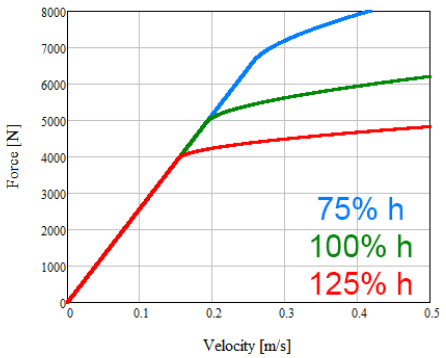

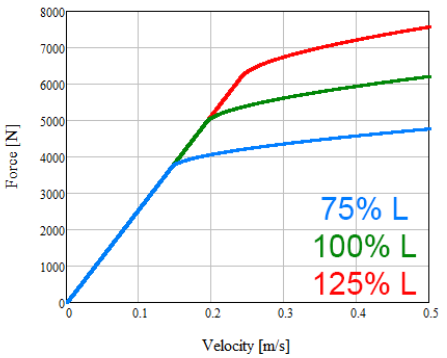

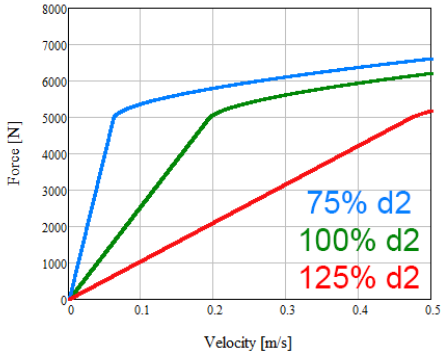

Experimental strut

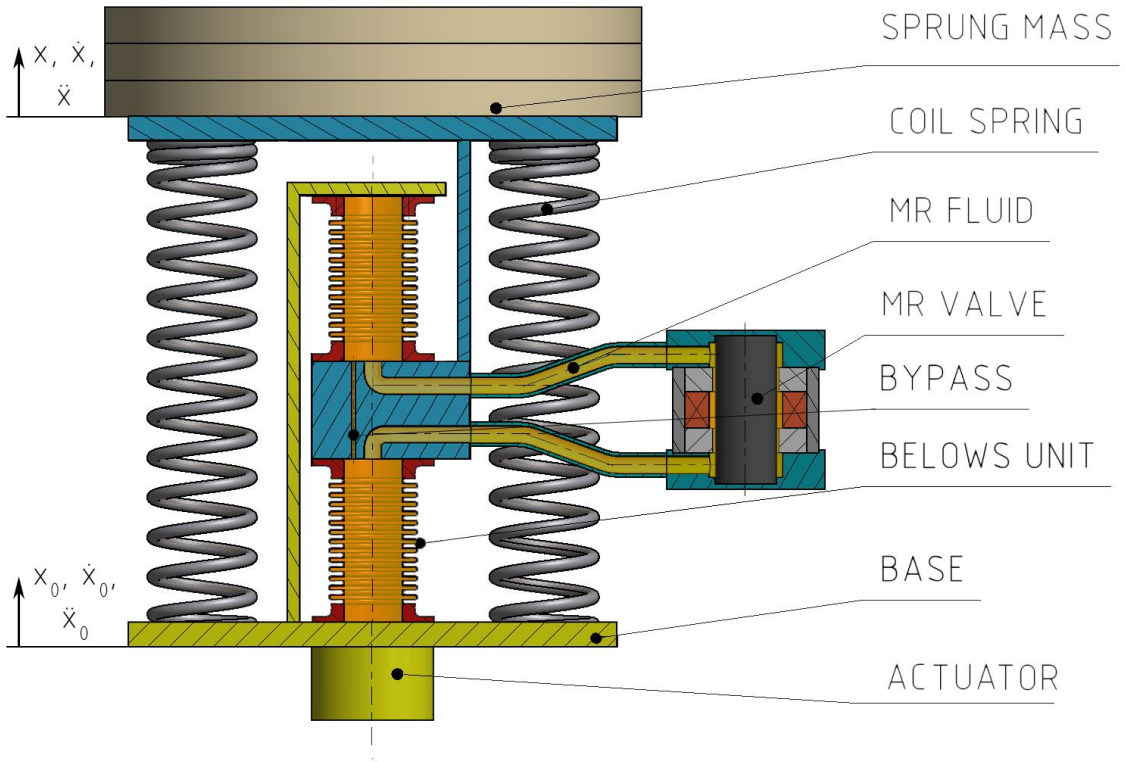

Bellows unit

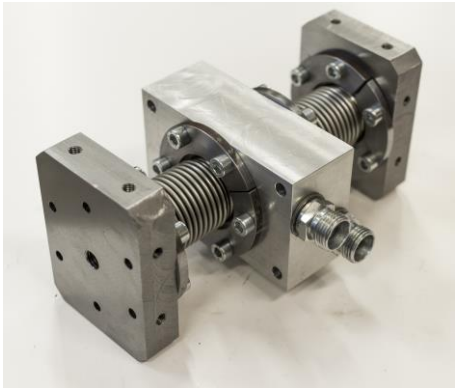

MR valve (Dr. Kubík)

Controller (Dr. Strecker)

Measurement of MR valve

Methods

Force – velocity dependency
+
Dynamic range

D = 9

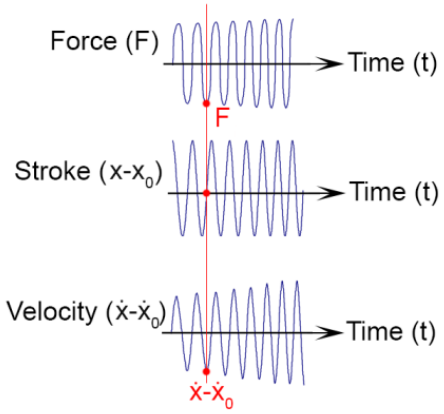

Time response

t = 4 ms

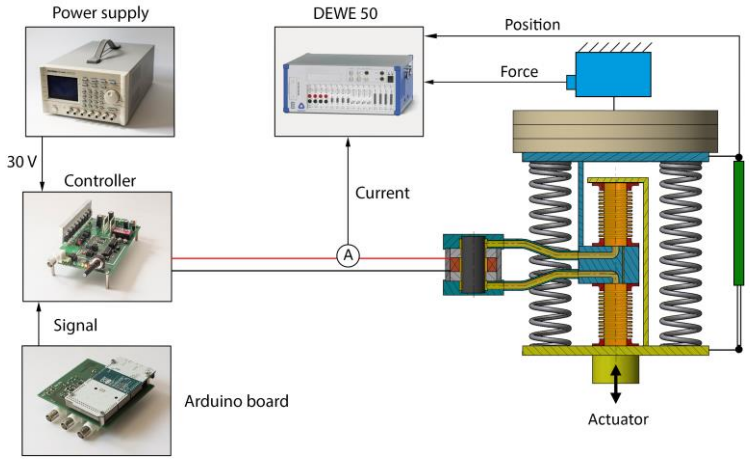

Results

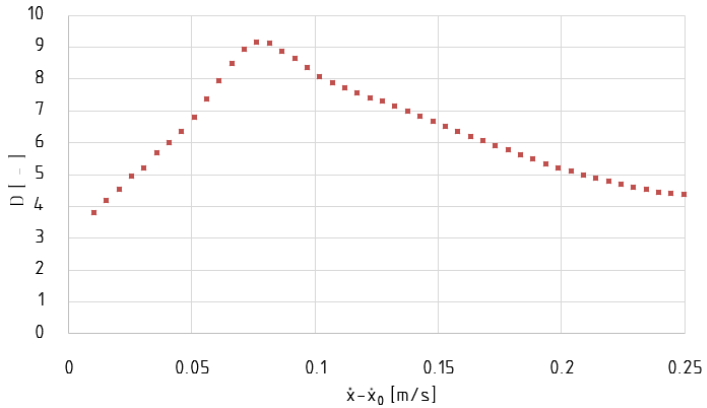

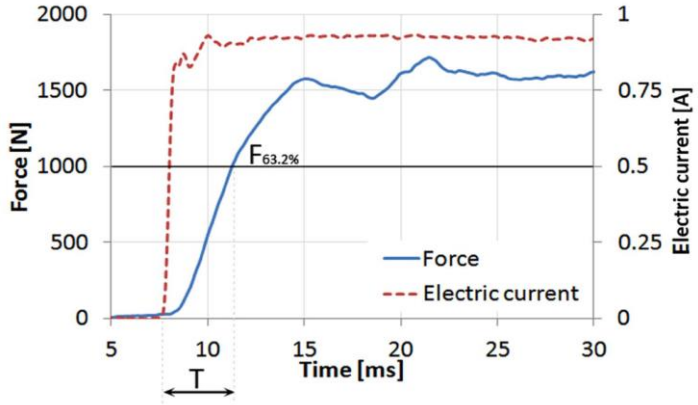

Demonstrator

Payload acceleration (response)

Relative displacement - > velocity (control)

Base acceleration (excitation)

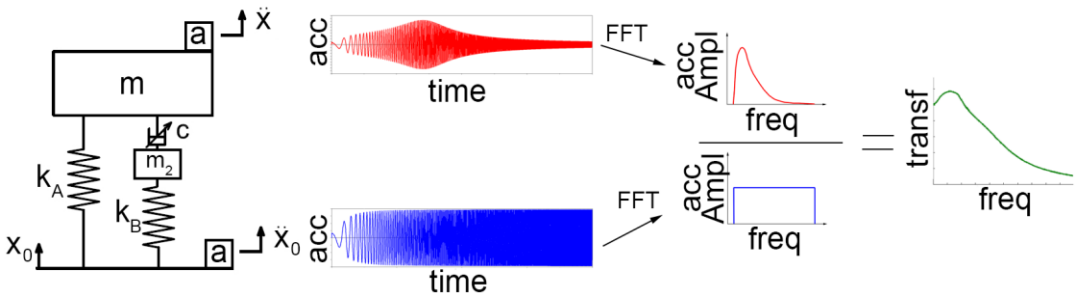

Measurement results

Transmissibility of experimental MR strut

Semi-active
(ON/OFF skyhook)
D = 9, t = 4 ms

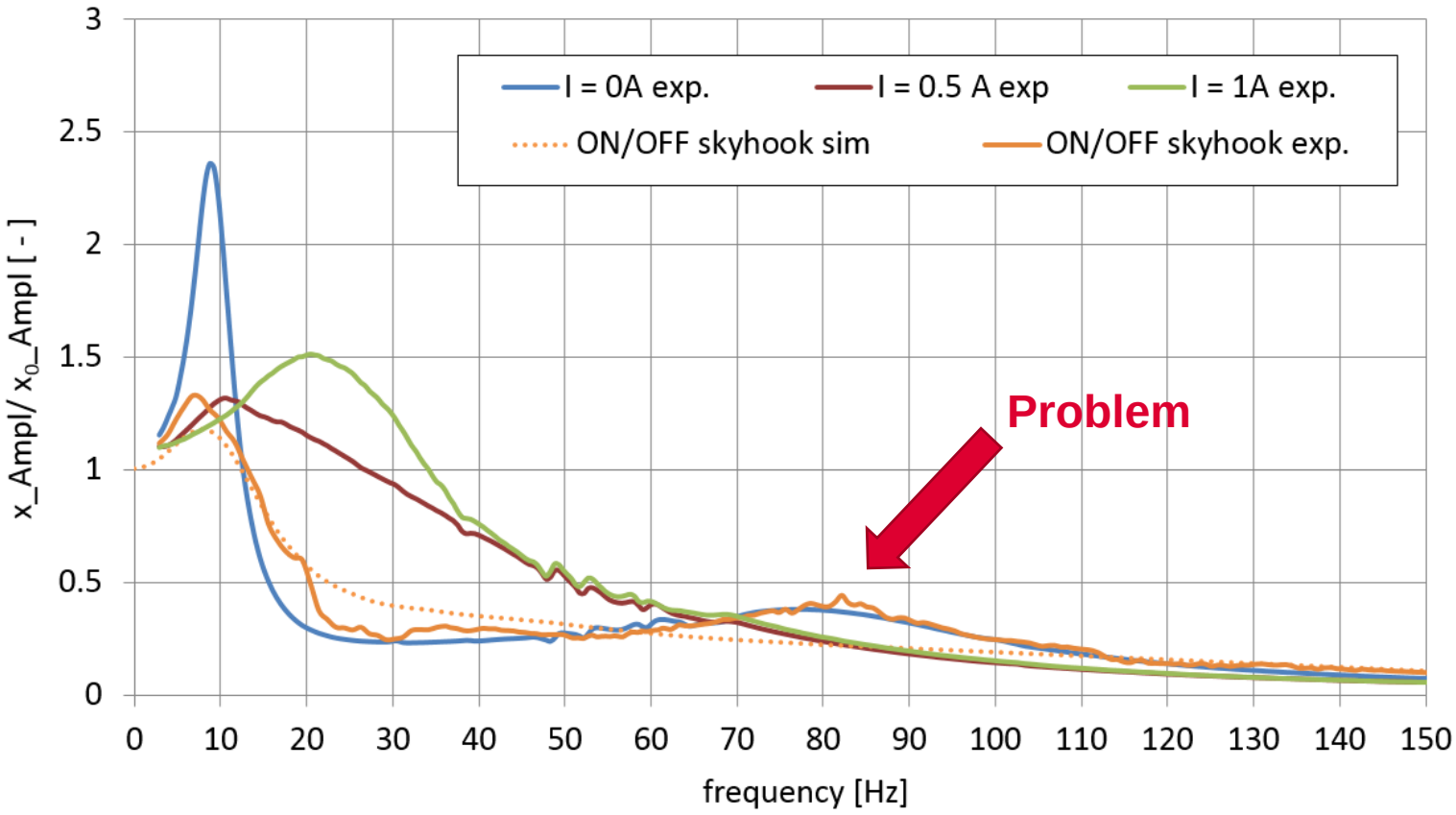

Measurement results

Conclusion of measurement of experimental MR strut

Cause of second peak:

mass effect – fluid mass oscillation in elastic casing

$$f = \frac{\sqrt{\frac{k_t}{m_f}}}{2 \cdot \pi}$$

$$\frac{1}{k_t} = \frac{1}{k} + \frac{1}{k_1}$$

$$m_f = \rho \cdot V$$

Configuration	Counting [Hz]	Measurement [Hz]	Deviation [%]
Multi-layer, MRF 139 EG	146.9	117.8	25
Single-layer, MRF 132 DG	115.2	78.6	47
Single-layer, oil	209.6	203.1	3

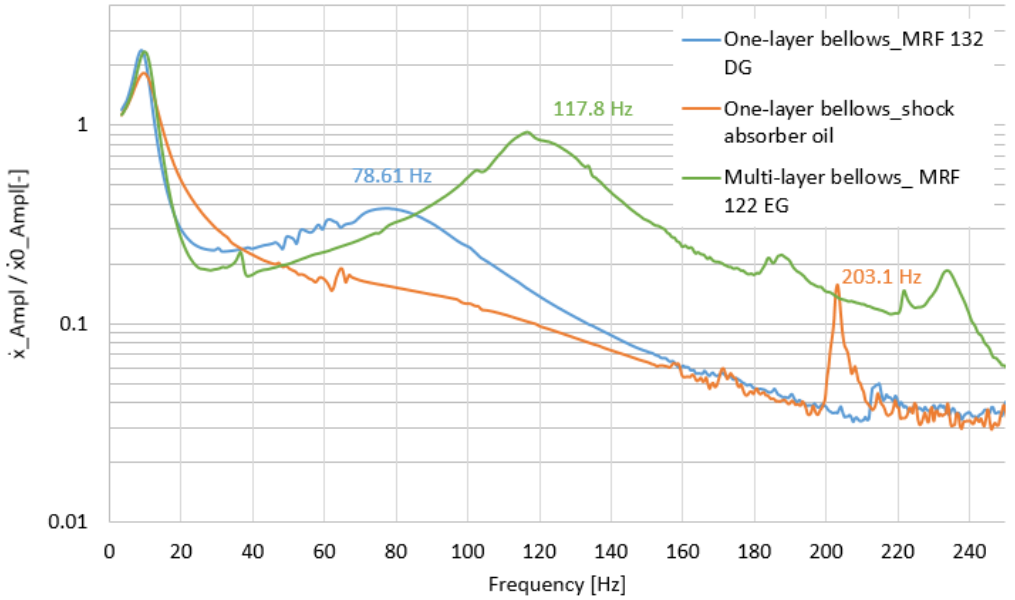

Minimize the fluid mass

Low volume, low concetration of iron

Measurement results

Conclusion of measurement of experimental MR strut

Ferrite rings cracked:

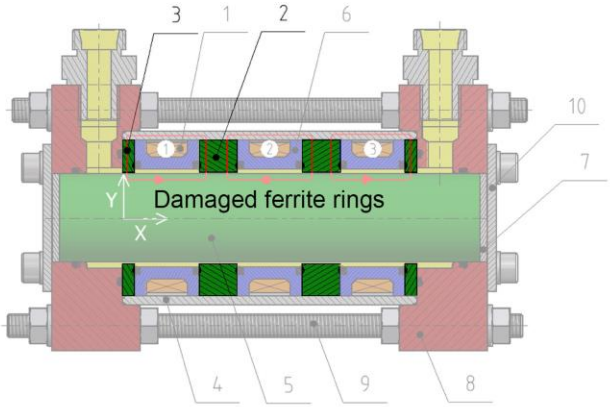

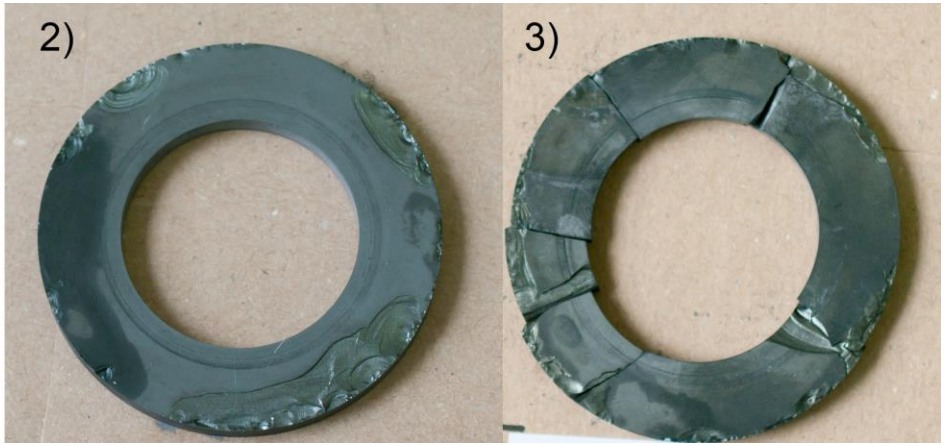

Material approach

↓

Shape approach

Design of MR for VIS of launch vehicle

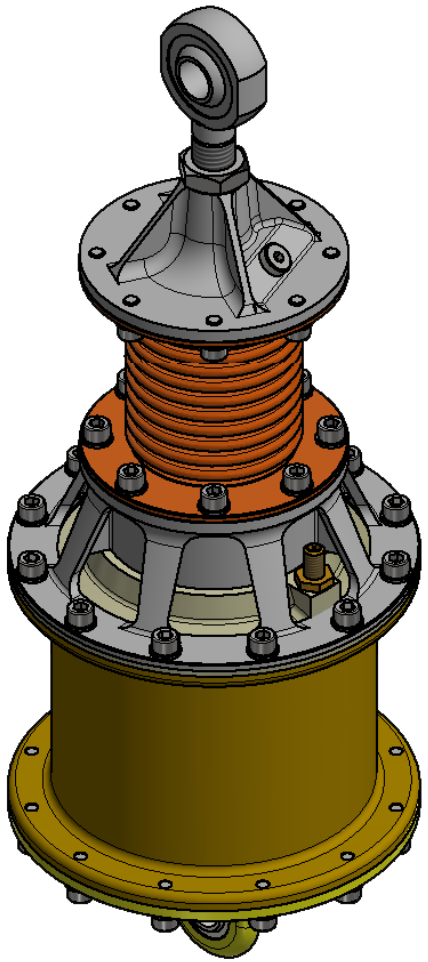

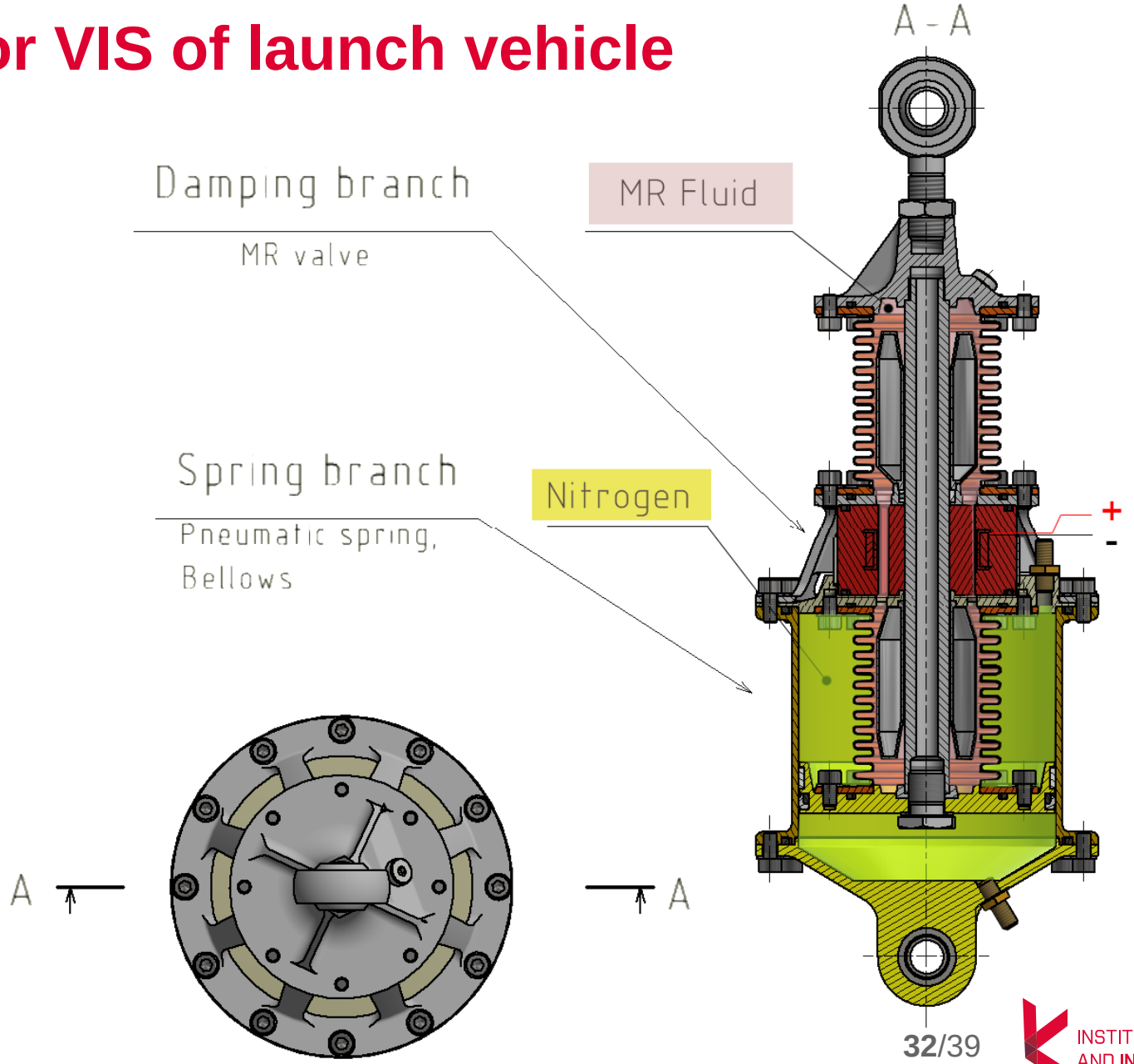

MR valve design

Magnetic part

Goal – Minimize eddy current to achieve fast time response of MR valve

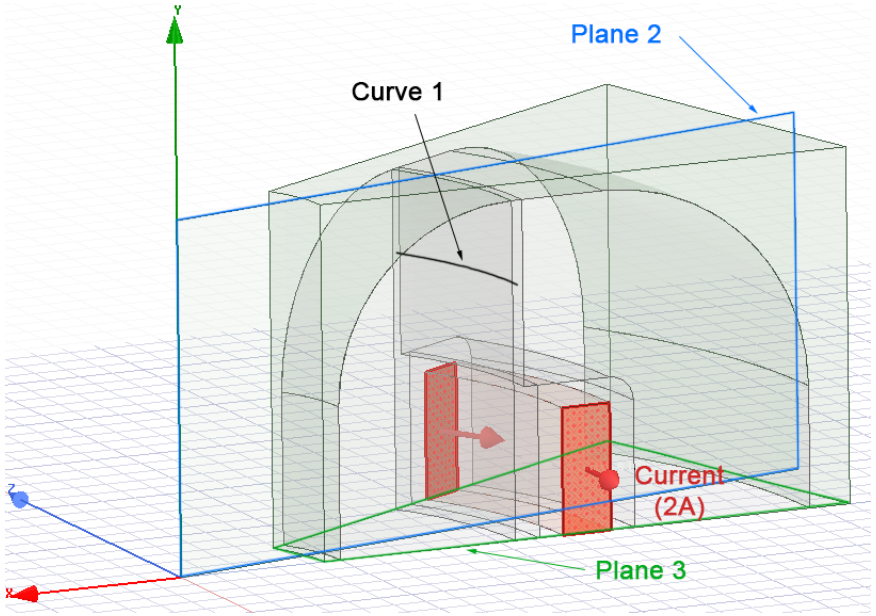

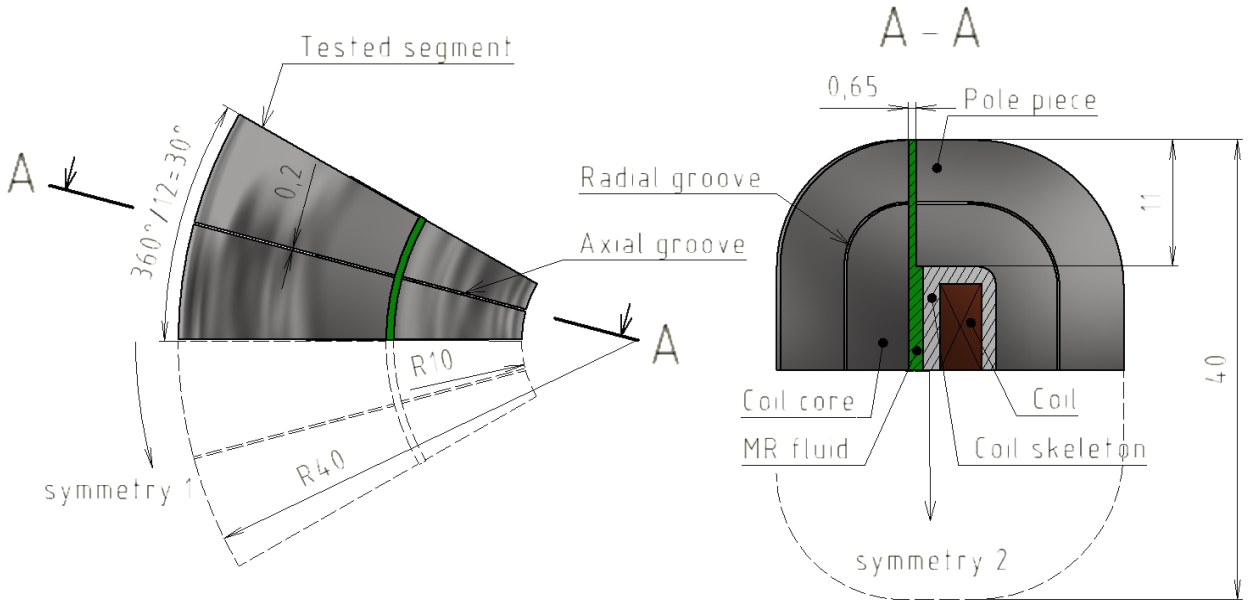

MR valve design

Eddy current in the magnetic circuit

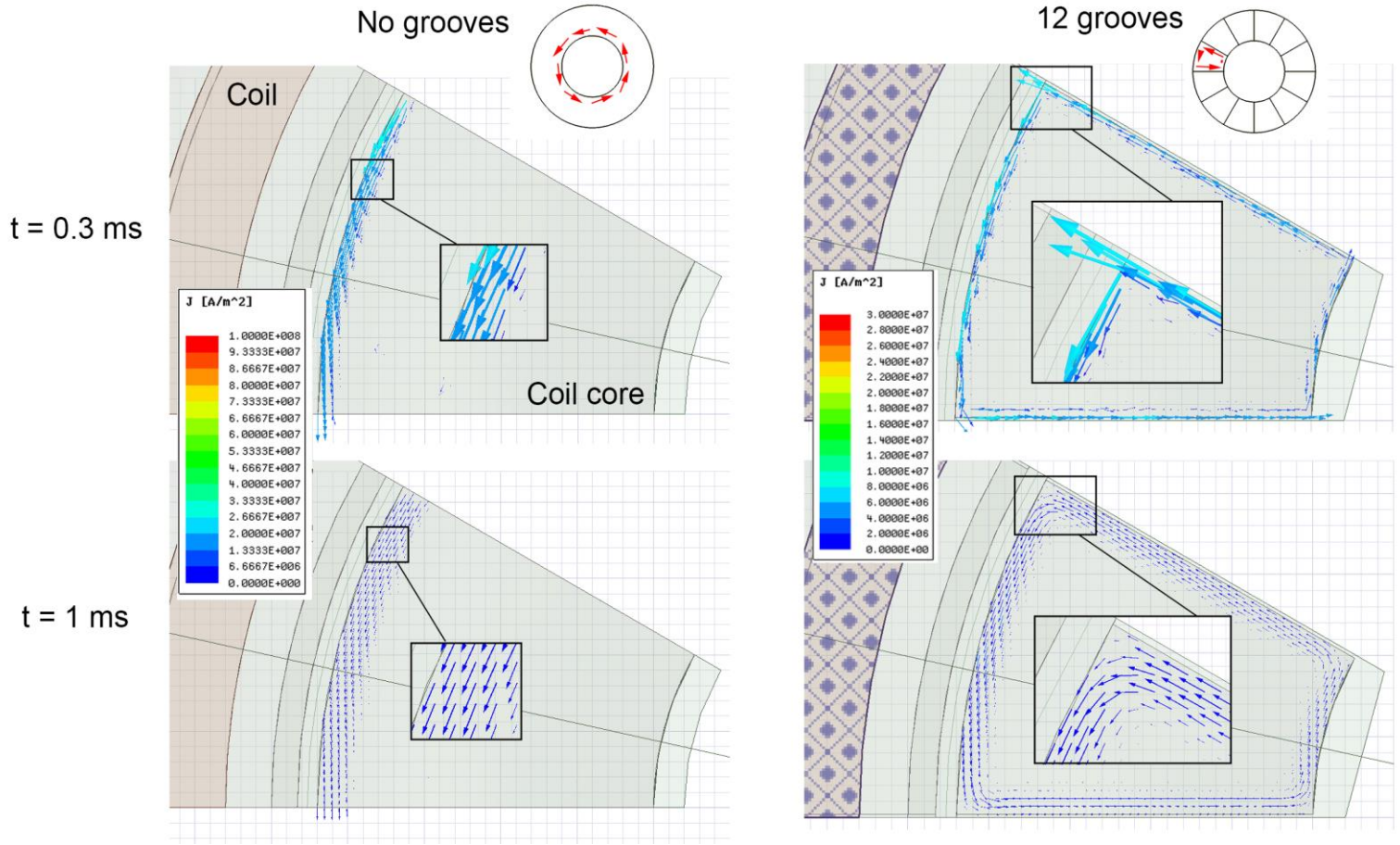

MR valve design

The magnetic circuit evolution

- Number of grooves
- Shape of grooves

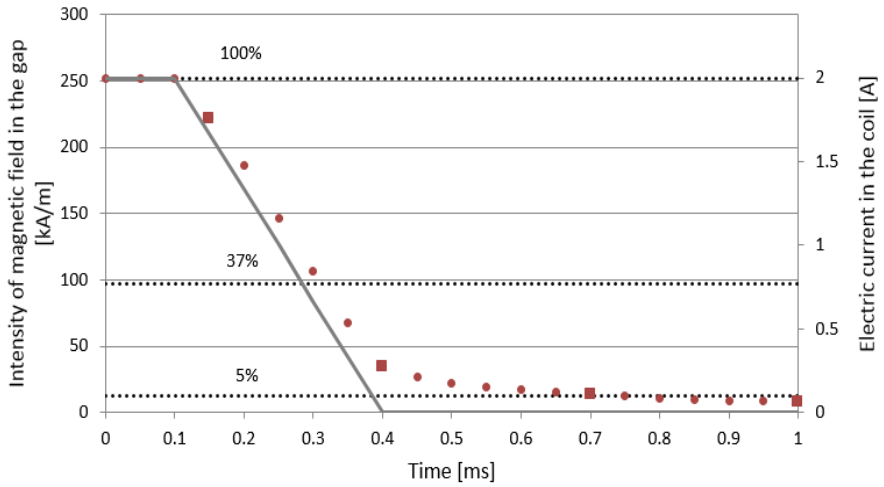

Time response of MR fluid: approx 0.6 ms

[Goncalves, 2005]

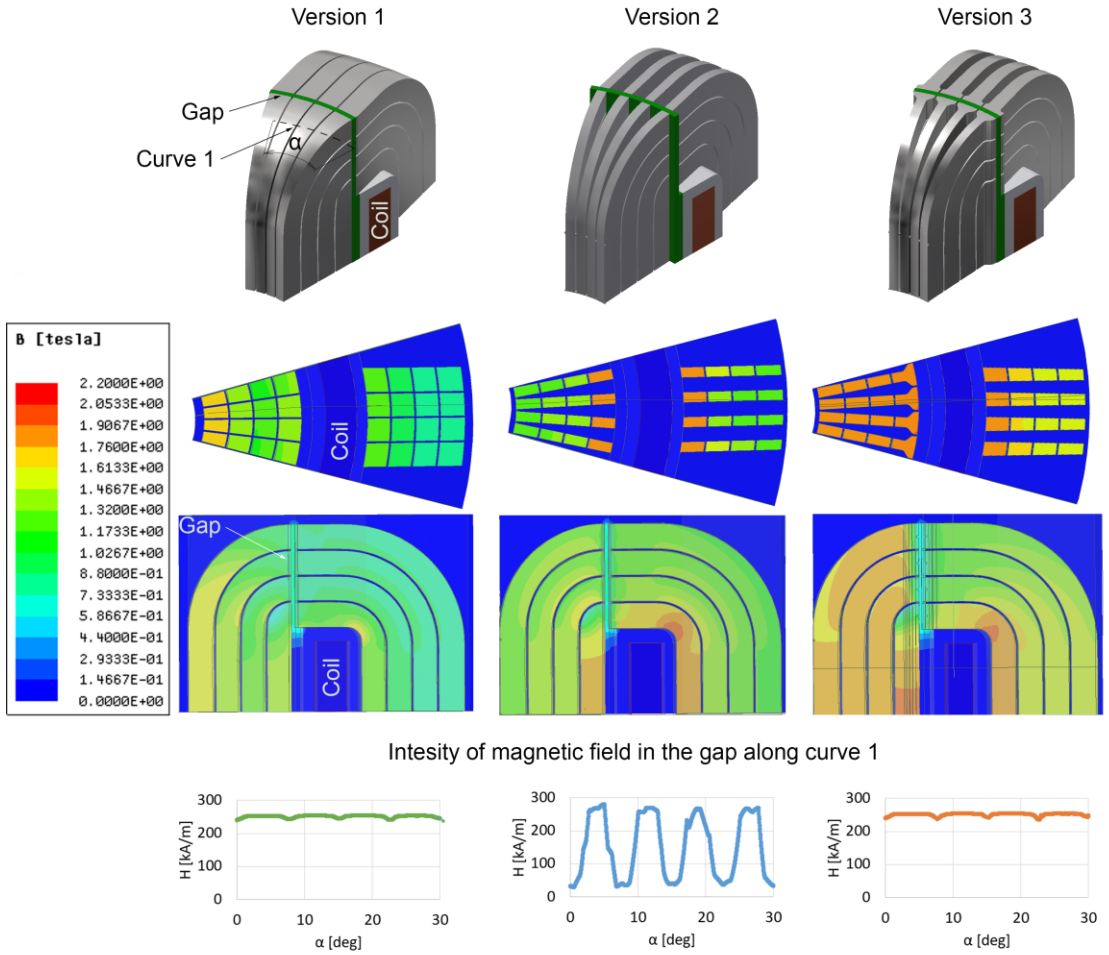

MR valve design

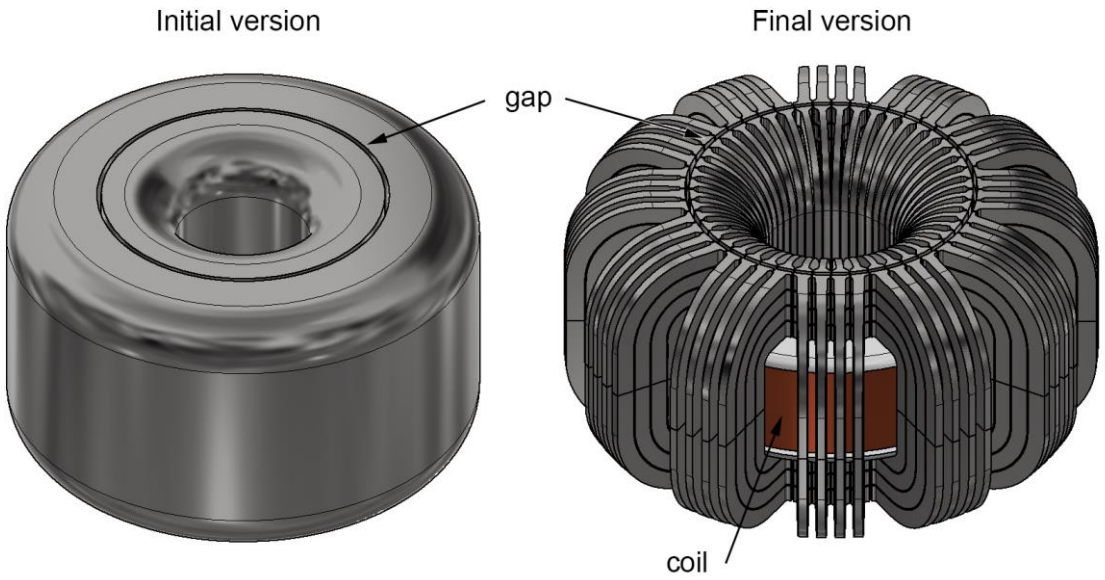

Version	Weight [kg]	Outer diameter [mm]	Primary time response [ms]	Secondary time response [ms]	Intensity of mag. field in the gap [kA/m]
Initial	1.184	69	3.84	15 (approx.)	264
Final	0.632	80	0.39	0.65	251
Difference	-46.6%	+15.9%	-94.3%		-4.6%

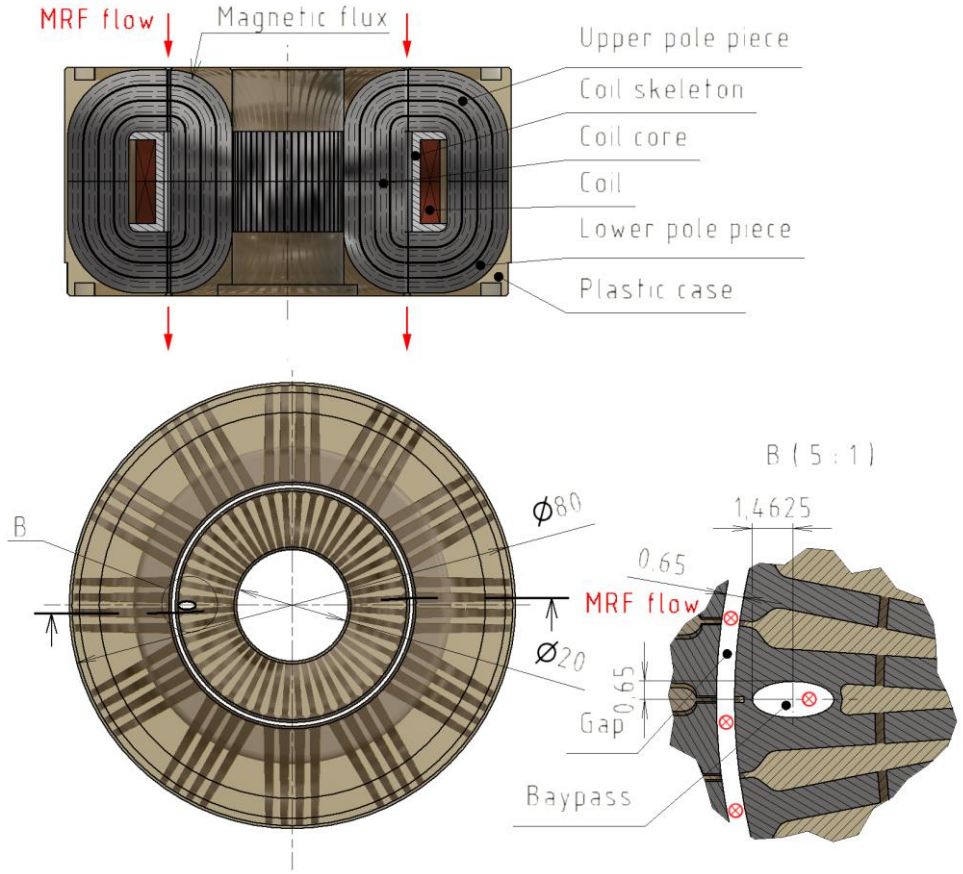

MR strut design

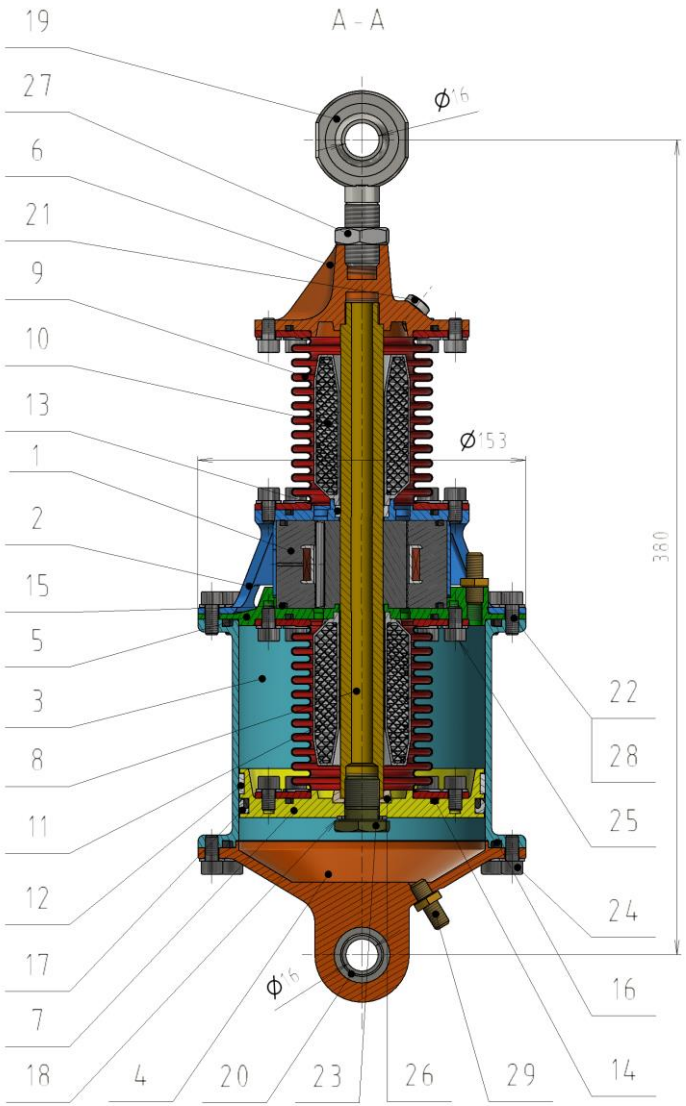

Pos.	Name of part	Material	Weight [g]	Quantity
1	MR valve	Vacoflux / Lukopren / cooper	693	1
2	MR valve body	AZ80A-T5 (magnesium alloy)	169	1
3	Cylinder	AZ80A-T5	337	1
4	Lid	AZ80A-T5	395	1
5	Flange	AZ80A-T5	159	1
6	Adapter	Ti6Al4V (titanium alloy)	279	1
7	Piston	AZ80A-T5	176	1
8	Piston rod	Ti6Al4V	230	1
9	Bellows	1.4571 (stainless steel)	447	2
10	Upper stopper	AZ80A-T5	49	1
11	Lower stopper	AZ80A-T5	48	1
12	Piston guideline	PTFE	2	1
13	Piston rod guideline	PTFE	11	1
14	Seal 66x2.5	NBR	1	4
15	Seal 71x2.5	NBR	2	2
16	Seal 123x3.4	NBR	4	2
17	Piston seal	NBR / PTFE	9	1
18	Bonded seal	NBR / Steel	2	1
19	Rod end M81935/1	Ti6Al4V	127	1
20	Lower mount	Ti6Al4V	16	1
21	Plug	AZ80A-T5 / NBR	2	1
39	Screw M6x16	Ti6Al4V	4	12
23	Piston rod screw	Ti6Al4V	23	1
24	Screw M6x12	Ti6Al4V	3	12
25	Screw M6x10	Ti6Al4V	3	32
26	Washer	Ti6Al4V	8	1
27	Nut	Ti6Al4V	12	1
28	Split washer 6.4	Ti6Al4V	0.4	56
29	Taxer valve	C-360 (brass alloy)	9	2
	MR Fluid	MR 122 EG	443	186 ml

Previous version of the strut with external MR valve had 8.03 kg

Total strut mass **4.145 kg**

Conclusion

Two versions of MR strut were designed

- Experimental – result were published in

KUBÍK, M.; MACHÁČEK, O.; STRECKER, Z.; ROUPEC, J.; MAZŮREK, I. Design and testing of magnetorheological valve with fast force response time and great dynamic force range. Smart Materials and Structures, 2017. 26(4), 47002. ISSN 0964-1726 IF 2.963

STRECKER, Z.; MAZŮREK, I.; ROUPEC, J.; MACHÁČEK, O.; KUBÍK, M. Influence of Response Time of Magnetorheological Valve in Skyhook Controlled Three-Parameter Damping System. Advances in Mecahnical Engineering. IF 0.864

MACHÁČEK, O.; KUBÍK, M.; STRECKER, Z.; ROUPEC, J.; MAZŮREK, I. Design of Frictionless Magnetorheological Damper with High Dynamic Force Range. Advances in Mecahnical Engineering. (after 3rd revision) IF 0.864

MACHÁČEK, O.; KUBÍK, M.; MAZŮREK, I.; STRECKER, Z.; ROUPEC, J. Frictionless Bellows Unit Connected with the Magnetorheological Valve. In Engineering Mechanics 2016. Praha: Institute of Thermomechanics Academy of Sciences of the Czech Republic, 2016. p. 354-357. ISBN: 978-80-87012-59- 8. (WoS)

- For the launch vehicle → The Method of design can by used also in other field of application

Time response of MR damper is the most important parameter in view of SA control → MACHÁČEK, O.; KUBÍK, M.; NOVÁK, P. A New Method of Magnetorheological Damper Quality Evaluation. In Engineering Mechanics 2017. Praha: Institute of Thermomechanics Academy of Sciences of the Czech Republic, 2017. p. 594-597. ISBN: 978-80-214-5497-2. (WoS)

Method of the pressure thrust stiffness determination was created → MACHÁČEK, O.; KUBÍK, M.; STRECKER, Z.; ROUPEC, J.; NOVÁK, P.; MAZŮREK, I. Axial and Pressure Thrust Stiffness of Metal Bellows for Vibration Isolators. In MATEC Web of Conferences. MATEC Web of Conferences. 2018. p. 1-5. ISSN: 3861-236X. (Scopus)

3D print can be used for ultra fast MR dampers → KUBÍK M.; MACHÁČEK O.; STRECKER Z.; ROUPEC J.; MAZUREK I.; KOUTNY D.; PALOUŠEK D., 2017. A Core Skeleton Made of Rods of Ferromagnetic Material. 307249, 2018. (European patent)

Thank you for your attention

Ondřej Macháček

ondrej.machacek@vutbr.cz

INSTITUTE OF **MACHINE**
AND **INDUSTRIAL DESIGN**

www.**ustavkonstruovani**.cz